Received 19 April 2024; revised 24 May 2024; accepted 13 June 2024. Date of publication 19 June 2024; date of current version 30 July 2024.

Digital Object Identifier 10.1109/OJCOMS.2024.3416467

Optimal Zak-OTFS Receiver and Its Relation to the Radar Matched Filter

SWAROOP GOPALAM (Member, IEEE), HAZER INALTEKIN (Member, IEEE), IAIN B. COLLINGS (Fellow, IEEE), AND STEPHEN V. HANLY (Fellow, IEEE)

School of Engineering, Macquarie University, Sydney, NSW 2113, Australia

CORRESPONDING AUTHOR: S. V. HANLY (e-mail: stephen.hanly@mq.edu.au)

This work was supported by the Australian Research Council's Discovery Project Funding Scheme under Project DP230102252.

ABSTRACT This paper presents optimal receiver implementations for Zak-OTFS modulation. Zak-OTFS has a receiver structure that includes a twisted convolution filter followed by delay-Doppler domain sampling. We first show that this receiver is equivalent to a correlation demodulator where the receive pulses are determined by the choice of the receive delay-Doppler domain twisted convolution (TC) filter. We formulate the notion of a matched TC filter as the receive TC filter that maximizes the SNR in an additive white Gaussian noise (AWGN) channel, for a given transmit TC filter. We show that the matched TC filter formulation is crucial for understanding noise processes in the delay-Doppler domain. More generally, for a doubly dispersive channel, we define a receive TC filter that is matched to the twisted convolution of the channel with the transmit TC filter. We show that this receive TC filter, sampled at the delay-Doppler grid points is the optimal Zak-OTFS receiver that recovers sufficient statistics for maximum likelihood detection of the data symbols. We first present an implementation of this optimal receiver for a general sparse doubly dispersive channel which requires radar matched filter processing and involves computing ambiguity functions. We then present a second implementation that uses a receive TC filter that is matched to the transmit TC filter (not the channel) and only requires time and frequency windowing. We show that these two approaches converge when the window supports are large relative to the fundamental periods of the delay-Doppler grid. We also show that the second approach has an interpretation as a rake receiver operating in the delay-Doppler domain.

INDEX TERMS Optimal receiver, delay-Doppler domain, Zak-OTFS, Zak transform, twisted convolution filters, time-frequency windowing, crystalline regime, rake receiver, channel predictability.

I. INTRODUCTION

ORTHOGONAL Time Frequency Space (OTFS) modulation was proposed for doubly dispersive channels to overcome the inter-carrier interference (ICI) problem suffered by OFDM in high Doppler scenarios [1], [2]. The core idea of OTFS is to modulate information symbols in the delay-Doppler (DD) domain, by using pulses which are nearly localized in the DD domain [1], [2], [3]. The sparsity of the DD domain channel is exploited to perform equalization efficiently [3], [4], [5], [6]. The original proposal of OTFS, referred to as multi-carrier OTFS (MC-OTFS), was a two stage implementation [2], where the OTFS symbol was created via a sequence of coded OFDM symbols. This provided a practical implementation, however it resulted in a complicated input-output relationship in which each information symbol undergoes a different transformation due to the channel, as was shown in [7], [8].

Recently in [7], [8], a new OTFS framework, called Zak-OTFS, was presented which directly uses the basis functions of the Zak transform for modulation. Zak-OTFS introduced the concept of a twisted convolution (TC) filter for DD domain pulse shaping of the waveform, which then leads to an input-output relationship where each symbol undergoes the same transformation through the channel. This allows for more accurate and simpler channel estimation and an ability to operate in non-sparse channels. It was also shown that the Zak-OTFS framework has the potential to offer superior bit error rate (BER) performance compared to MC-OTFS

in high Doppler spread scenarios. In [9], it was shown that Zak-OTFS has superior performance over an alternative multi-carrier modulation based DD domain scheme called Orthogonal Delay Doppler Modulation (ODDM) [10] and MC-OTFS in terms of out-of-band emissions and channel predictability.

In [9], practical implementations of Zak-OTFS modulation were proposed, which included implementation of TC filters and generation of the time domain Zak-OTFS waveform. Time and frequency windowing functions were proposed to implement two different classes of DD domain TC filters (called Type-1 and Type-2) [9]. It was shown that the Zak-OTFS transmitter for a Type-1 transmit TC filter can be implemented via a Time Division Multiplexing (TDM) pulse shaping approach, and for a Type-2 transmit TC filter, it can be implemented via an Orthogonal Frequency Division Multiplexing (OFDM) pulse shaping approach, after necessary precoding and digital windowing steps. The previously known Discrete Zak Transform (DZT) based OTFS implementation [11] is a special case of Type-1 Zak-OTFS when restricting to a rectangular time window, and the DD-OFDM modulation [12] is a special case of Type-2 Zak-OTFS when both frequency and time windows are rectangular.

Zak-OTFS has a receiver structure that includes a twisted convolution filter followed by delay-Doppler domain sampling. Existing Zak-OTFS receiver implementations rely on time and frequency windowing based TC filters, and they sample on the DD grid points [8], [9], [11]. The question of an optimal Zak-OTFS receiver which recovers the sufficient statistics for maximum likelihood detection, remains open. In this paper, we present optimal Zak-OTFS receiver structures that are crucial for realizing the full potential of this new DD domain modulation scheme.

First, we show that a Zak-OTFS receiver is equivalent to a correlation demodulator with underlying receive pulses which are determined by the receive TC filter. For a given transmit TC filter, we formulate the notion of a matched TC filter at the receiver and show that it maximizes the SNR in an AWGN channel (analogous to a matched filter in pulse amplitude modulation, *i.e.,* time division multiplexing). The matched TC filter formulation is crucial for understanding noise processes in the DD domain. We characterize the white noise process as a non-stationary Gaussian process in the DD domain. We show that filtering white noise with a TC filter also results in a Gaussian process and that specifying its covariance function requires the notion of a matched TC filter.

More generally, for a doubly dispersive channel, we define a receive TC filter that is matched to the twisted convolution of the channel with the transmit TC filter. We show that this receive TC filter, sampled at the delay-Doppler grid points is the optimal Zak-OTFS receiver that recovers sufficient statistics for maximum likelihood detection of the data symbols. We show that this optimal Zak-OTFS receiver is closely linked to a radar matched filtering approach for a single radar target channel. A similar link was recently noted for the discrete DD domain, in the context of channel tap estimation [13].

We present two implementations of the optimal receiver for general sparse doubly dispersive channels, based on the insight from the single radar target channel. The first receiver implementation requires radar matched filter processing and involves computing ambiguity functions. The second implementation uses matched Type-1 and Type-2 transmit and receive filters, and only requires appropriate time and frequency windowing of the received signal followed by DD domain sampling via the discrete Zak transform. We show that this Type-1 and Type-2 based Zak-OTFS implementation converges to the optimal radar matched filter approach, in the crystalline regime, *i.e.,* when the window supports are larger than the fundamental periods of the delay-Doppler grid. We also show that the proposed Type-1 and Type-2 based Zak-OTFS approach has an interpretation as a rake receiver operating in the delay-Doppler domain.

Our results for radar sensing using Type-1 and Type-2 Zak-OTFS pulsones show that a Zak-OTFS receiver can be directly used for radar sensing with no performance loss in terms of SNR, delay resolution, or Doppler resolution, compared to the standard radar approach, when operating in the crystalline regime. These results emphasise the suitability of Zak-OTFS as a candidate waveform for integrated sensing and communication.

In summary, the contributions of the paper are as follows:

- In Section III, we derive results on the Zak-OTFS receiver structure and introduce the concept of a matched TC filter.
- In Section IV, we show that noise processes are DD domain Gaussian processes.
- In Section V, we derive the structure of the optimal Zak-OTFS receiver for doubly dispersive channels.
- In Section VI, we derive the effective channel response of Type-1 and Type-2 Zak-OTFS implementations, where the receiver is matched to the transmit TC filter.
- In Section VII, we compare a Type-1 and Type-2 Zak-OTFS implementation with a radar matched filtering approach for radar sensing in a single target channel, and also reveal connections to the optimal Zak-OTFS receiver.
- In Section VIII, we present implementations of the optimal Zak-OTFS receiver.

II. ZAK-OTFS SYSTEM MODEL

This section summarizes the essential framework of Zak-OTFS modulation that was introduced in [7], [8], and also the time and frequency windowing based Zak-OTFS implementation introduced in [9]. In the following sections, we will present receiver structures for this system model. Note that the receiver implementations in prior work [7], [8], [9], [11], [12] used time-frequency based TC filtering with DD grid sampling. The optimality, or otherwise, of that approach was not addressed. In Section VIII, we will

derive the optimal Zak-OTFS receiver for doubly dispersive channels, using general TC filtering. We also provide implementations underpinned by fractional sampling.

A. ZAK-OTFS MODULATION

Zak-OTFS modulates data in the delay-Doppler domain, where both delay and Doppler are discretized on a $M \times N$ grid. The data symbols $\hat{x}[l,k]$ are placed on the $M \times N$ DD data grid, where $0 \leq l \leq M-1$ is the delay index and $0 \leq k \leq N-1$ is the Doppler index. The conversion to DD domain from the time domain is done through the Zak transform as defined below [7].

Definition 1: For $T > 0$, the Zak transform of a continuous time signal $s(t)$ is defined as

$$\mathcal{Z}_s(\tau, \nu) \coloneqq \sum_{n \in \mathbb{Z}} s(\tau + nT) e^{-j2\pi\nu nT}. \tag{1}$$

$\mathcal{Z}_s(\tau,\nu)$ is the delay-Doppler domain representation of the time domain signal $s(t)$.

Note that a DD domain signal is quasi-periodic due to the quasi-periodicity of the Zak transform, *i.e.,* $\mathcal{Z}_s(\tau + n'T, \nu + m'\Delta f) = e^{j2\pi\nu n'T}\mathcal{Z}_s(\tau,\nu)$ for each $m', n' \in \mathbb{Z}$ and $\Delta f \coloneqq \frac{1}{T}$.

1) ZAK-OTFS TRANSMITTER

As shown in [7], the full Zak-OTFS discrete DD domain signal $x_{\mathrm{dd}}[l',k']$ is constructed by performing a quasi periodic encoding of the data symbols onto the infinite DD grid, by extending the $M \times N$ data grid as follows:

$$x_{\mathrm{dd}}[l + nM, k + mN] \coloneqq \hat{x}[l,k] e^{j2\pi \frac{nk}{N}} \tag{2}$$

for $(m,n) \in \mathbb{Z}\times\mathbb{Z}$ and $(l,k) \in \{0,\ldots,M-1\}\times\{0,\ldots,N-1\}$.

The discrete signal $x_{\mathrm{dd}}[l',k']$ is then converted to an analog DD domain signal $x_{\mathrm{dd}}(\tau,\nu)$[1] on the grid, by modulating the discrete values using DD domain impulses, as follows:

$$x_{\mathrm{dd}}(\tau,\nu) \coloneqq \sum_{(l',k') \in \mathbb{Z}\times\mathbb{Z}} x_{\mathrm{dd}}[l',k'] \delta\left(\tau - \frac{l'T}{M}\right)\delta\left(\nu - \frac{k'\Delta f}{N}\right). \tag{3}$$

Hence, the impulse at location $(l'\frac{T}{M}, k'\frac{\Delta f}{N})$ modulates the symbol $x_{\mathrm{dd}}[l',k']$ for each $(l',k') \in \mathbb{Z}\times\mathbb{Z}$.

It was proposed in [7] that the pulse shaping of the signal $x_{\mathrm{dd}}(\tau,\nu)$ in Zak-OTFS be done by means of a DD domain twisted convolution (TC) filter [7], where the twisted convolution operation of two DD domain functions is defined as follows:

Definition 2: Twisted convolution of two DD functions $a(\tau,\nu)$, $b(\tau,\nu)$ is defined as

$$a *_\sigma b(\tau,\nu) \coloneqq \iint a(\tau',\nu') b(\tau - \tau', \nu - \nu') e^{j2\pi\nu'(\tau-\tau')} d\tau' d\nu'.$$

[1]Note that the DD domain Zak-OTFS signal $x_{\mathrm{dd}}(\tau,\nu)$ is a quasi-periodic DD function. Quasi-periodicity is crucial since all time domain signals are quasi-periodic DD domain functions under the Zak transform. Other arbitrary DD functions do not correspond to time domain signal representations.

Remark 1: As noted before, all time domain signals correspond to quasi-periodic functions in the DD domain, and as noted in [7], [8], twisted convolution operations preserve quasi-periodicity. Hence, the resulting output of a DD domain TC filter corresponds to a time domain signal.[2]

Let $g(\tau,\nu)$ denote a generic TC filter in the DD domain. Now let $g^{\mathrm{Tx}}(\tau,\nu)$ specifically denote the transmit filter of Zak-OTFS. The transmitted DD domain signal in Zak-OTFS is therefore given by $x_{\mathrm{dd}}^{g^{\mathrm{Tx}}}(\tau,\nu) \coloneqq g^{\mathrm{Tx}} *_\sigma x_{\mathrm{dd}}(\tau,\nu)$. By Remark 1, the DD domain signal $x_{\mathrm{dd}}^{g^{\mathrm{Tx}}}(\tau,\nu)$ can be converted to the time domain transmitted signal using the inverse Zak transform as

$$x(t) \coloneqq \frac{1}{\Delta f}\int_0^{\Delta f} x_{\mathrm{dd}}^{g^{\mathrm{Tx}}}(t,\nu) d\nu. \tag{4}$$

The transmit TC filter is critical for Zak-OTFS waveform implementation.[3] Section II-B, provides details of the transmit TC filters and the corresponding time domain transmitted signal $x(t)$.

The following two subsections discuss the effect of the channel in the DD domain, and the Zak-OTFS DD domain receiver processing, which are crucial for our subsequent derivation of the optimal Zak-OTFS receiver.

2) DOUBLY DISPERSIVE CHANNEL

The output of the channel, *i.e.,* the received time domain signal is given by

$$y(t) = r(t) + n(t) \tag{5}$$

where $n(t)$ is the additive noise, and the signal component

$$r(t) \coloneqq \iint h(\tau,\nu) x(t-\tau) e^{j2\pi\nu(t-\tau)} d\tau d\nu \tag{6}$$

where $h(\tau,\nu)$ is the delay-Doppler response (also known as delay-Doppler spreading function) of the doubly dispersive channel. Taking the Zak-transform of (6), results in a twisted convolution relation [8] in the DD domain as

$$\mathcal{Z}_r(\tau,\nu) = h *_\sigma \mathcal{Z}_x(\tau,\nu) = h *_\sigma \left(g^{\mathrm{Tx}} *_\sigma x_{\mathrm{dd}}\right)(\tau,\nu) \tag{7}$$

where (7) follows from the fact that the transmitted DD signal $\mathcal{Z}_x(\tau,\nu)$ is the transmit TC filtered version of $x_{\mathrm{dd}}(\tau,\nu)$.

3) ZAK-OTFS RECEIVER AND EFFECTIVE CHANNEL RESPONSE

As proposed in [7], at the receiver, a receive TC filter $g^{\mathrm{Rx}}(\tau,\nu)$ is applied to the received signal $\mathcal{Z}_y(\tau,\nu)$ to obtain the TC filtered received signal $y_{\mathrm{dd}}(\tau,\nu) \coloneqq g^{\mathrm{Rx}} *_\sigma \mathcal{Z}_y(\tau,\nu)$. Substituting $\mathcal{Z}_r(\tau,\nu)$ from (7), the effective DD domain input-output (I/O) relation of Zak-OTFS is obtained as

$$y_{\mathrm{dd}}(\tau,\nu) = h_{\mathrm{dd}}(\tau,\nu) *_\sigma x_{\mathrm{dd}}(\tau,\nu) + n_{\mathrm{dd}}(\tau,\nu) \tag{8}$$

[2]see Definition 3 for the time domain expression of a TC filtered signal.

[3]For a detailed treatment of Zak-OTFS time domain transmitter implementations, see [9], which includes a comparison of various transmit TC filters and their resource efficiency in terms of bandwidth and time duration.

where $n_{\rm dd}(\tau,\nu)$ is the receive TC filtered noise process and the effective DD channel response [7] is given by

$$h_{\rm dd}(\tau,\nu) \coloneqq g^{\rm Rx} *_\sigma h *_\sigma g^{\rm Tx}(\tau,\nu) \tag{9}$$

is a cascade of three TC filters, 1) transmit TC filter, 2) the channel response and 3) receive TC filter.

As shown in [7], [8], the discrete DD domain samples are obtained by sampling the TC filtered received signal $y_{\rm dd}(\tau,\nu)$ on the DD grid points $(\tau,\nu) = (l\frac{T}{M}, k\frac{\Delta f}{N})$ for $(l,k) \in \mathbb{Z}\times\mathbb{Z}$ to obtain

$$y_{\rm dd}[l,k] = y_{\rm dd}\left(l\frac{T}{M}, k\frac{\Delta f}{N}\right). \tag{10}$$

Note that quasi-periodicity of the Zak-transform means that $y_{\rm dd}[l+nM, k+mN] = y_{\rm dd}[l,k]e^{j2\pi\frac{nk}{N}}$ for all $(m,n) \in \mathbb{Z}^2$. Hence, knowledge of the MN samples $\{y_{\rm dd}[l',k']\}$ for $(l',k') \in \{0,\ldots,M-1\}\times\{0,\ldots,N-1\}$ at the receiver is sufficient, since these samples contain all the information of the infinite 2D sequence $y_{\rm dd}[l,k]$ for any $(l,k) \in \mathbb{Z}^2$.

B. ZAK-OTFS IMPLEMENTATION IN THE TIME DOMAIN USING TYPE-1 AND TYPE-2 TC FILTERS

This subsection summarizes the Zak-OTFS implementation framework in [9] including Type-1 and Type-2 TC filters. In the following sections, we will show that one of our optimal Zak-OTFS receiver designs can be implemented using these TC filters.

Definition 3: In the time domain, TC filtering of a signal $s(t)$ with a TC filter $g(\tau,\nu)$ is equivalent to the following operation:

$$s^g(t) \coloneqq \iint g(\tau,\nu)s(t-\tau)e^{j2\pi\nu(t-\tau)}d\tau d\nu, \tag{11}$$

i.e., $\mathcal{Z}_{s^g}(\tau,\nu) = g *_\sigma \mathcal{Z}_s(\tau,\nu)$ in the DD domain. We use the notation $s^g(t)$ and $g *_\sigma s(t)$ in the time domain to represent the signal $s(t)$ TC filtered by $g(\tau,\nu)$, to indicate that the relationship in the DD domain is a twisted convolution.

1) TYPE-1 AND TYPE-2 TC FILTERS

We focus on the two general classes of TC filters (Type-1 and Type-2) proposed in [9]. Type-1 filters are a product of a delay spreading function, $\alpha(\tau)$, and a Doppler spreading function, $\beta(\nu)$, as follows:

$$g_1(\tau,\nu) = \alpha(\tau)\beta(\nu) \tag{12}$$

and Type-2 filters have an extra multiplicative sinusoidal component as follows:

$$g_2(\tau,\nu) = \alpha(\tau)\beta(\nu)e^{j2\pi\tau\nu} \tag{13}$$

Let $A(f)$ denote the *frequency window* which is the Fourier transform of delay component $\alpha(\tau)$ and $B(t)$ denote the *time window* which is the inverse Fourier transform of Doppler component $\beta(\nu)$, defined as follows:

$$A(f) \coloneqq \int \alpha(\tau)e^{-j2\pi f\tau}d\tau \tag{14}$$

$$B(t) \coloneqq \int \beta(\nu)e^{j2\pi\nu t}d\nu. \tag{15}$$

The key result of [9] concerning time-frequency windowing is summarized in the following note. This note shows that twisted convolution operation in the DD domain with Type-1 and Type-2 TC filters is equivalent to frequency windowing (*i.e.,* convolution in time) and time windowing operations with window functions $A(f), B(t)$ in the appropriate order.

Note 1: From [9, Th. 1];

- Applying time window $B(t)$ followed by frequency window $A(f)$ on a signal $s(t)$ is equivalent to TC filtering with Type-1 TC filter $g_1(\tau,\nu)$ in the DD domain, *i.e.,*

$$s^{g_1}(t) = \alpha(t) * (B(t)s(t)) \tag{16}$$

$$\mathcal{Z}_{s^{g_1}}(\tau,\nu) = g_1 *_\sigma \mathcal{Z}_s(\tau,\nu) \tag{17}$$

  where $*$ represents convolution.
- Applying frequency window $A(f)$ followed by time window $B(t)$ on a signal $s(t)$ is equivalent to TC filtering with Type-2 TC filter $g_2(\tau,\nu)$ in the DD domain, *i.e.,*

$$s^{g_2}(t) = B(t)(\alpha(t) * s(t)) \tag{18}$$

$$\mathcal{Z}_{s^{g_2}}(\tau,\nu) = g_2 *_\sigma \mathcal{Z}_s(\tau,\nu) \tag{19}$$

  where $*$ represents convolution.

2) TIME DOMAIN TRANSMIT PULSES CORRESPONDING TO TYPE-1 AND TYPE-2 TC FILTERS

The key result of [9] regarding Zak-OTFS transmit pulses is summarized in the following note. First, we introduce the necessary terminology and notation.

The unfiltered Zak-OTFS transmit pulse corresponding to point (τ,ν) is defined as

$$\phi_{\tau,\nu}(t) \coloneqq T\sum_{n\in\mathbb{Z}} e^{j2\pi\nu nT}\delta(t-\tau-nT) \tag{20}$$

We also denote

$$\tau_l \coloneqq l\frac{T}{M} \text{ and } \nu_k \coloneqq k\frac{\Delta f}{N} \tag{21}$$

for $(l,k) \in \mathbb{R}\times\mathbb{R}$ to be the normalized representation of points on the DD domain plane, where the normalization is with respect to grid resolution $(\frac{T}{M}, \frac{\Delta f}{N})$.

As noted in [9], these unfiltered transmit pulses correspond to the DD domain signal $x_{\rm dd}(\tau,\nu)$ (from (3)) as it is the Zak-transform of $\sum_{l=0}^{M-1}\sum_{k=0}^{N-1}\hat{x}[l,k]\phi_{\tau_l,\nu_k}(t)$.

Note 2: In [9], it was shown that

- The time domain Zak-OTFS transmit pulses $\{\phi^{g_1}_{\tau_l,\nu_k}(t)\}$ that modulate data symbols $\hat{x}[l,k]$ for $(l,k) \in \{0,\ldots,M-1\}\times\{0,\ldots,N-1\}$, corresponding to Type-1 transmit TC filter $g_1(\tau,\nu)$ are

$$\phi^{g_1}_{\tau_l,\nu_k}(t) = T\sum_{n\in\mathbb{Z}} B(\tau_l+nT)e^{j2\pi\nu_k nT} \alpha(t-\tau_l-nT) \tag{22}$$

  which is a train of pulses $\{\alpha(t-\tau_l-nT)\}_{n\in\mathbb{Z}}$ modulating samples of a time windowed tone $B(t')e^{j2\pi\nu_k(t'-\tau_l)}$ sampled at pulse locations $t' = \tau_l + nT$.

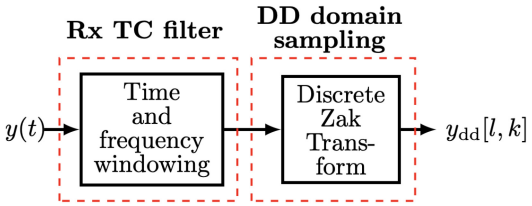

FIGURE 1. Block Diagram of a time and frequency windowing based Zak-OTFS receiver.

- The time domain Zak-OTFS transmit pulses $\{\phi^{g_2}_{\tau_l,\nu_k}(t)\}$ that modulate data symbols $\hat{x}[l,k]$ for $(l,k) \in \{0,\ldots,M-1\}\times\{0,\ldots,N-1\}$, corresponding to Type-2 transmit TC filter $g_2(\tau,\nu)$ are

$$\phi^{g_2}_{\tau_l,\nu_k}(t) = B(t)e^{j2\pi\nu_k(t-\tau_l)} \sum_{m\in\mathbb{Z}} A(m\Delta f+\nu_k)e^{j2\pi m\Delta f(t-\tau_l)} \quad (23)$$

  which is the product of a periodic pulse train $\sum_{m\in\mathbb{Z}} A(m\Delta f+\nu_k)e^{j2\pi m\Delta f(t-\tau_l)}$ and a time windowed tone $B(t)e^{j2\pi\nu_k(t-\tau_l)}$.

As noted in [9], these TC filtered transmit pulses correspond to the pulse shaped (*i.e.,* TC filtered) DD domain signal $x^{g^{\rm Tx}}_{\rm dd}(\tau,\nu)$, since the corresponding transmit signal $x(t)$ (from (4)) equals $\sum_{l=0}^{M-1}\sum_{k=0}^{N-1}\hat{x}[l,k]\phi^{g^{\rm Tx}}_{\tau_l,\nu_k}(t)$.

For Type-1 and Type-2 transmit TC filters, note that the time window $B(t)$ determines the time duration of Zak-OTFS signal, and the frequency window $A(f)$ determines the bandwidth, as was shown in [9]. For detailed implementations see [9], where it was shown that the Type-2 Zak-OTFS transmitter has an OFDM based implementation whereas the Type-1 transmitter has a TDM based implementation, with additional precoding and digital windowing steps.

As explained in Note 2, the Type-1 and Type-2 Zak-OTFS transmit pulses consist of two components, a pulse train component, and a windowed tone component. Hence, these Zak-OTFS transmit pulses are also referred to as *pulsones* [7].

3) ZAK-OTFS RECEIVER IMPLEMENTATION USING TIME AND FREQUENCY WINDOWING

As shown in [9], the implementation of a Zak-OTFS receiver for a Type-1 or a Type-2 receive TC filter is done according to the block diagram in Figure 1. This Zak-OTFS receiver consists two blocks, a receive TC filter block which performs frequency and time windowing of the signal, and a DD domain sampling block that use discrete Zak transform (DZT) to obtain DD domain samples from the time domain samples.

For the first block, note that for a Type-1 or a Type-2 receive filter $g^{\rm Rx}(\tau,\nu)$, the TC filtering operation can be performed by time windowing and frequency windowing in the appropriate order, given in Note 1. The resulting signal in the DD domain is

$$\mathcal{Z}_{y^{g^{\rm Rx}}}(\tau,\nu) = g^{\rm Rx} *_\sigma \mathcal{Z}_y(\tau,\nu) = y_{\rm dd}(\tau,\nu). \quad (24)$$

To obtain the output symbols $y_{\rm dd}[l,k]$, from $y^{g^{\rm Rx}}(t)$ (or equivalently $y_{\rm dd}(\tau,\nu)$ as shown above), the DZT block is implemented as follows:

$$y_{\rm dd}[l,k] = \mathcal{Z}_{y^{g^{\rm Rx}}}(\tau_l,\nu_k) = \sum_{n\in Z} y^{g^{\rm Rx}}(nT+\tau_l)e^{-j2\pi\nu_k nT} = \sum_{n\in Z} y^{g^{\rm Rx}}\left((nM+l)\frac{T}{M}\right)e^{-j2\pi\frac{nk}{N}} \quad (25)$$

where (25) follows from the definition of Zak transform in (1). As in (25), the output symbols $y_{\rm dd}[l,k]$ are obtained from the time domain samples (taken at integer multiples of $\frac{T}{M}$, *i.e.,* at a sampling rate $M\Delta f$) of the receive TC filtered signal $y^{g^{\rm Rx}}(t)$, using the DZT operation.

III. ZAK-OTFS RECEIVER STRUCTURE AND THE MATCHED TWISTED CONVOLUTION FILTER

In this section, we introduce our notion of a matched TC filter and derive its structure. The matched TC filter formulation will be crucial for deriving the optimal Zak-OTFS receiver, and for characterizing noise processes in the DD domain.

We first show that a general Zak-OTFS receiver (for an arbitrary receive TC filter) is equivalent to a correlation demodulator where the underlying receive pulses are determined by the choice of the receive TC filter. We then use this insight to introduce the matched TC filter.

A. ZAK-OTFS RECEIVER AS A CORRELATION DEMODULATOR

We now present an alternative interpretation of a general Zak-OTFS receiver (*i.e.,* for a general receive TC filter) as a *correlation demodulator*. We show that the underlying receive pulses of Zak-OTFS are determined by its choice of the receive TC filter.

Note that the Zak transform from (1) can be alternatively expressed using basis functions as follows:

$$\mathcal{Z}_s(\tau,\nu) := \int s(t)\psi_{\tau,\nu}(t)dt \quad (26)$$

where the Zak transform basis function $\psi_{\tau,\nu}(t)$, parameterized by delay variable τ and Doppler variable ν, is

$$\psi_{\tau,\nu}(t) := \frac{\phi^*_{\tau,\nu}(t)}{T} = \sum_{n\in Z}\delta(t-\tau-nT)e^{-j2\pi\nu nT} \quad (27)$$

We use this interpretation of the Zak transform, *i.e.,* (26)-(27), in Theorem 1, which is our main result on the Zak-OTFS receive pulses.

Theorem 1: For a general receive TC filter $g(\tau,\nu)$, the output of the Zak-OTFS receiver sampled at (τ',ν'), *i.e.,*

$$\mathcal{Z}_{y^g}(\tau',\nu') := \int (g *_\sigma y(t))\ \psi_{\tau',\nu'}(t)dt$$

is equivalent to a correlation receiver that correlates $y(t)$ with the receive pulse that is a TC filtered version of the Zak transform basis function as follows:

$$\mathcal{Z}_{y^g}(\tau',\nu') = \int y(t)\ \left(\tilde{g} *_\sigma \psi_{\tau',\nu'}(t)\right)dt, \quad (28)$$

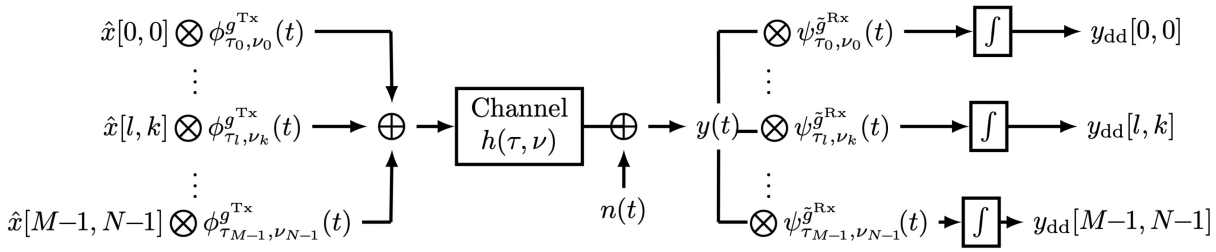

FIGURE 2. A general Zak-OTFS receiver as a correlator demodulator: The transmitter modulates data symbols $\hat{x}[l,k]$ on the transmit pulses $\phi^{g^{\mathrm{Tx}}}_{\tau_l,\nu_k}(t)$. At the receiver, the DD domain samples $y_{\mathrm{dd}}[l,k]$ are the correlation outputs of the received signal $y(t)$ with the receive pulses $\psi^{\tilde{g}^{\mathrm{Rx}}}_{\tau_l,\nu_k}(t)$.

where the TC filter $\tilde{g}(\tau,\nu)$ is defined as

$$\tilde{g}(\tau,\nu) \coloneqq g(-\tau,\nu)e^{j2\pi\nu\tau}. \tag{29}$$

Proof: See Appendix A. ■

Remark 2: In Theorem 1, we have shown that, for a signal $y(t)$ and a TC filter $g(\tau,\nu)$, a Zak transform sample $\mathcal{Z}_{y^g}(\tau',\nu')$ of the TC filtered signal (evaluated at point (τ',ν')) is equivalent to taking the correlation of the original signal $y(t)$ with the TC filtered Zak-transform basis function $\psi^{g}_{\tau',\nu'}(t)$.

Hence, a Zak-OTFS receiver is equivalent to a correlation demodulator as illustrated in Figure 2. The transmitter consists of MN pulses $\{\phi^{g^{Tx}}_{l,k}(t)\}$ that are determined by the choice of the transmit TC filter. The receiver consists of a bank of MN correlators with underlying receive pulses $\{\psi^{\tilde{g}^{Rx}}_{l,k}(t)\}$ that are determined by the choice of the receive TC filter.

For the case of Type-1 and Type-2 receive TC filters, we obtain the main result on the Zak-OTFS receive pulses as a corollary of Theorem 1 as follows:

Corollary 1: For $(l,k) \in \{0,\ldots,M-1\} \times \{0,\ldots,N-1\}$, the received symbol $y_{dd}[l,k]$ is determined as follows:

- For a Type-1 TC filter $g_1(\tau,\nu) = \alpha(\tau)\beta(\nu)$, $y_{dd}[l,k] = \int y(t)\psi^{\tilde{g}_1}_{\tau_l,\nu_k}(t)dt$, where the receive pulse is

$$\psi^{\tilde{g}_1}_{\tau_l,\nu_k}(t) \coloneqq \Delta f\ B(t)e^{-j2\pi\nu_k(t-\tau_l)} \sum_{m\in Z} A(\nu_k + m\Delta f)\ e^{-j2\pi m\Delta f(t-\tau_l)}. \tag{30}$$

- For a Type-2 TC filter $g_2(\tau,\nu) = \alpha(\tau)\beta(\nu)e^{j2\pi\nu\tau}$, $y_{dd}[l,k] = \int y(t)\psi^{\tilde{g}_2}_{\tau_l,\nu_k}(t)dt$, where the receive pulse is

$$\psi^{\tilde{g}_2}_{\tau_l,\nu_k}(t) \coloneqq \sum_{n\in\mathbb{Z}} B(\tau_l + nT)e^{-j2\pi\nu_k nT} \alpha(\tau_l + nT - t). \tag{31}$$

Remark 3:

- By inspection of (23) and (30), note that the Type-1 receive pulse has the same pulsone structure as a Type-2 transmit pulse. More precisely, let $g^{Tx}(\tau,\nu) \coloneqq \alpha(\tau)\beta(\nu)e^{j2\pi\nu\tau}$ be the Type-2 transmit TC filter, and let $g^{Rx}(\tau,\nu) = \alpha^*(-\tau)\beta^*(-\nu)$ be the Type-1 TC filter associated with the conjugate frequency window $A^*(f)$ and the conjugate time window $B^*(t)$. Then,

$$T\psi^{\tilde{g}^{Rx}}_{\tau_l,\nu_k}(t) = \left(\phi^{g^{Tx}}_{\tau_l,\nu_k}(t)\right)^*. \tag{32}$$

- By inspection of (22) and (31), note that the Type-2 receive pulse has the same pulsone structure as a Type-1 transmit pulse. More precisely, let $g^{Tx}(\tau,\nu) \coloneqq \alpha(\tau)\beta(\nu)$ be the Type-1 transmit TC filter, and let $g^{Rx}(\tau,\nu) = \alpha^*(-\tau)\beta^*(-\nu)e^{j2\pi\nu\tau}$ be the Type-2 TC filter associated with the conjugate frequency window $A^*(f)$ and the conjugate time window $B^*(t)$. Then,

$$T\psi^{\tilde{g}^{Rx}}_{\tau_l,\nu_k}(t) = \left(\phi^{g^{Tx}}_{\tau_l,\nu_k}(t)\right)^*. \tag{33}$$

From Remark 3, when a Type-1 transmit TC filter is combined with a Type-2 receive TC filter, the transmit pulse and the receive pulse have the same structure. Furthermore, if conjugate windows are used at the receiver, the receive pulses are conjugates of the transmit pulses.

Hence, we focus on two Zak-OTFS implementations that can be implemented using time and frequency windowing, as in Figure 1. We call them, Type-1 Zak-OTFS and Type-2 Zak-OTFS. In a Type-1 Zak-OTFS implementation, the transmit TC filter is of Type-1 and the receive TC filter is of Type-2 (with conjugate windows). In a Type-2 Zak-OTFS, the transmit TC filter is of Type-2 and the receive TC filter is of Type-1 (with conjugate windows). Table 1 summarizes the details of the TC filters under the two implementations,

TABLE 1. Type-1 and Type-2 Zak-OTFS implementations.

	Transmit TC Filter $g^{\mathrm{Tx}}(\tau,\nu)$	**Receive TC Filter** $g^{\mathrm{Rx}}(\tau,\nu)$
Type-1 Zak-OTFS	Type-1 TC Filter $\alpha(\tau)\beta(\nu)$	Type-2 TC Filter $\alpha^*(-\tau)\beta^*(-\nu)e^{j2\pi\nu\tau}$
Type-2 Zak-OTFS	Type-2 TC Filter $\alpha(\tau)\beta(\nu)e^{j2\pi\nu\tau}$	Type-1 TC Filter $\alpha^*(-\tau)\beta^*(-\nu)$

	Time and Frequency Windowing Operations at the Receiver
Type-1 Zak-OTFS	Frequency windowing with $A^*(f)$ followed by time windowing with $B^*(t)$.
Type-2 Zak-OTFS	Time windowing with $B^*(t)$ followed by frequency windowing with $A^*(f)$.

and the corresponding time-frequency windowing operations at the receiver.[4]

In the next subsection, we show that the proposed implementations have an interpretation as a *matched TC filter* in an additive white Gaussian noise channel.

B. MATCHED TWISTED CONVOLUTION FILTER

To characterize the optimal TC filter, we start with the simplest channel. Consider an additive white Gaussian noise (AWGN) channel as follows:

$$y(t) = s(t) + n(t), \tag{34}$$

where $s(t)$ is the input signal and $n(t)$ is an AWGN process whose noise power spectral density is N_0 Watts per Hz.

Suppose that the input signal $s(t)$ is the Zak-OTFS transmit pulse $\phi^{g^{\mathrm{Tx}}}_{\tau_l,\nu_k}(t)$ (for transmit TC filter $g^{\mathrm{Tx}}(\tau,\nu)$), where $\phi_{\tau_l,\nu_k}(t)$ is the unfiltered transmit pulse of Zak-OTFS from (20). Let $g^{\mathrm{Rx}}(\tau,\nu)$ denote the receive TC filter. The signal power of Zak-OTFS receiver output $y_{\mathrm{dd}}[l,k]$ is given by

$$\left|\mathcal{Z}_{s^{g^{\mathrm{Rx}}}}(\tau_l,\nu_k)\right|^2 = \left|\int \phi^{g^{\mathrm{Tx}}}_{\tau_l,\nu_k}(t)\psi^{\tilde{g}^{\mathrm{Rx}}}_{\tau_l,\nu_k}(t)dt\right|^2$$

by applying Theorem 1.

Since $n_{\mathrm{dd}}[l,k] = \int n(t)\psi^{\tilde{g}^{\mathrm{Rx}}}_{\tau_l,\nu_k}(t)dt$ from Theorem 1, the noise variance is given by

$$\sigma^2_{\tau_l,\nu_k} := \mathbb{E}\Big[|n_{\mathrm{dd}}[l,k]|^2\Big] = N_0\int\left|\psi^{\tilde{g}^{\mathrm{Rx}}}_{\tau_l,\nu_k}(t)\right|^2 dt,$$

obtained by using the fact that $\mathbb{E}[n(t)n^*(t+\tau)] = N_0\delta(\tau)$.

By Cauchy-Schwarz inequality,

$$\left|\mathcal{Z}_{s^{g^{\mathrm{Rx}}}}(\tau_l,\nu_k)\right|^2 \le \int\left|\phi^{g^{\mathrm{Tx}}}_{\tau_l,\nu_k}(t)\right|^2 dt\int\left|\psi^{\tilde{g}^{\mathrm{Rx}}}_{\tau_l,\nu_k}(t)\right|^2 dt$$

and hence the SNR must satisfy

$$\frac{\left|\mathcal{Z}_{s^{g^{\mathrm{Rx}}}}(\tau_l,\nu_k)\right|^2}{\sigma^2_{\tau_l,\nu_k}} \le \frac{\int\left|\phi^{g^{\mathrm{Tx}}}_{\tau_l,\nu_k}(t)\right|^2 dt}{N_0} \tag{35}$$

where the equality holds when $\psi^{\tilde{g}^{\mathrm{Rx}}}_{\tau_l,\nu_k}(t) = K(\phi^{g^{\mathrm{Tx}}}_{\tau_l,\nu_k}(t))^*$ for any constant $K \neq 0$.

Mirroring the definition of a matched filter, we define the notion of a *matched TC filter* as follows.

Definition 4: The matched twisted convolution filter of the transmit TC filter $g^{Tx}(\tau,\nu)$ is the receive TC filter $g^{Rx}(\tau,\nu)$ that achieves the maximum SNR in (35) for each l,k.

For a general transmit filter $g^{\mathrm{Tx}}(\tau,\nu)$, we derive the matched TC filter in the following theorem.

Theorem 2: For a transmit TC filter $g^{Tx}(\tau,\nu)$, the matched TC filter at the receiver is

$$g^{Rx}(\tau,\nu) = \Big(g^{Tx}(\tau,\nu)\Big)^\dagger := \Big(g^{Tx}(-\tau,-\nu)\Big)^* e^{j2\pi\nu\tau}. \tag{36}$$

[4]The transmitter implementation for Type-1 Zak-OTFS is provided in [9, Sec. V.A], whereas the transmitter implementation for Type-2 Zak-OTFS is provided in [9, Sec. V.B].

Furthermore, the receive pulse corresponding to the matched TC filter $g^{Rx}(\tau,\nu) = (g^{Tx}(\tau,\nu))^\dagger$ is

$$\psi^{\tilde{g}^{Rx}}_{\tau_l,\nu_k}(t) = \frac{1}{T}\Big(\phi^{g^{Tx}}_{\tau_l,\nu_k}(t)\Big)^*. \tag{37}$$

Proof: See Appendix A. ■

The receive TC filters presented in Remark 3 are matched to the Type-1 and Type-2 transmit TC filters as noted in the following corollary.

Corollary 2: For a Type-1 transmit TC filter, the matched receive TC filter is a Type-2 TC filter using conjugate windows. Similarly, for a Type-2 transmit TC filter, the matched receive TC filter is a Type-1 TC filter using conjugate windows.

Theorem 2 motivates the following definition of a *matched TC filter* operation on a DD domain function.

Definition 5: The matched TC filter operation, denoted by $(\cdot)^\dagger$, is defined as

$$a^\dagger(\tau,\nu) = a^*(-\tau,-\nu)e^{j2\pi\nu\tau} \tag{38}$$

for any DD domain function $a(\tau,\nu)$.

Property 1: Let $a(\tau,\nu)$ and $b(\tau,\nu)$ denote two arbitrary DD domain functions, we note the following properties of the matched TC filter operation $(\cdot)^\dagger$:

$$\Big(a^\dagger(\tau,\nu)\Big)^\dagger = a(\tau,\nu) \tag{39}$$

$$(a *_\sigma b)^\dagger(\tau,\nu) = b^\dagger *_\sigma a^\dagger(\tau,\nu) \tag{40}$$

From (39), operation $(\cdot)^\dagger$ is its own inverse. From (40), operation $(\cdot)^\dagger$ flips the order of functions in twisted convolution.

We will use these properties of the matched TC filter operation throughout the rest of the paper.

IV. CHARACTERIZATION OF NOISE PROCESSES IN THE DD DOMAIN

In this section, we show that noise processes in the DD domain are Gaussian processes, and we derive a DD domain input-output relationship for TC filtered white Gaussian noise. We derive its covariance function and show that it requires the notion of the matched TC filter (that we introduced in the previous section).

A. TC FILTERED NOISE PROCESS CHARACTERIZATION

Let $n(t)$ be a white Gaussian noise process with power spectral density N_0 Watts per Hz and let $n^g(t)$ denote the TC filtered noise process in the time domain where the TC filter is $g(\tau,\nu)$. We denote $\mathcal{Z}_{n^g}(\tau,\nu)$ to be the TC filtered white noise process $n^g(t)$ represented in the DD domain.

Definition 6: The noise covariance function of TC filtered DD domain noise process $\mathcal{Z}_{n^g}(\tau,\nu)$ is defined as

$$C_{\mathcal{Z}_{n^g}}(\tau,\nu|\tau',\nu') := \mathbb{E}\Big[\mathcal{Z}_{n^g}(\tau,\nu)\mathcal{Z}^*_{n^g}(\tau',\nu')\Big] \tag{41}$$

The noise covariance function is crucial for characterizing the distribution of the TC filtered noise process $\mathcal{Z}_{n^g}(\tau,\nu)$ in the DD domain.

Theorem 3: Suppose that the TC filtered basis functions $\psi^{\tilde{g}}_{\tau_\circ,\nu_\circ}(t)$ are square integrable for all $(\tau_\circ, \nu_\circ) \in \mathbb{R}^2$, for a given TC filter $g(\tau, \nu)$. Then, the following hold:

1) The DD domain TC filtered noise process $\mathcal{Z}_{n^g}(\tau, \nu)$ is a zero mean Gaussian process.
2) The covariance function of $\mathcal{Z}_{n^g}(\tau, \nu)$ is given by

$$C_{\mathcal{Z}_{n^g}}(\tau, \nu|\tau', \nu') = \frac{N_0}{T} g *_\sigma g^\dagger *_\sigma \mathcal{Z}_{\phi_{\tau',\nu'}}(\tau, \nu) \quad (42)$$

where $\phi_{\tau',\nu'}(t)$ is defined in (20) and its Zak transform is $\mathcal{Z}_{\phi_{\tau',\nu'}}(\tau, \nu) = \sum_{(m,n)\in\mathbb{Z}^2} e^{j2\pi\nu' nT}\delta(\tau-\tau'-nT)\delta(\nu-\nu'-m\Delta f)$.

Proof: See Appendix B. ∎

Remark 4: We note that our Theorem 3 completely characterizes the TC filtered noise process $\mathcal{Z}_{n^g}(\tau, \nu)$, since for zero mean Gaussian processes, the covariance function is sufficient to characterize the distributions (see [14, Th. 3.6.3]). Also note that $\mathcal{Z}_{n^g}(\tau, \nu)$ is a non-stationary Gaussian process in the DD domain since the covariance function $C_{\mathcal{Z}_{n^g}}(\tau, \nu|\tau', \nu')$ is not just a function of $\tau - \tau'$ and $\nu - \nu'$, but also depends on ν'.

B. TYPE-1 AND TYPE-2 TC FILTERED NOISE PROCESS

In this subsection, we focus on the case of Type-1 and Type-2 TC filters, and provide conditions on when the noise samples (and hence the received output samples) are uncorrelated.

We start by introducing the necessary terminology.

Definition 7:
- The cross-ambiguity function of two time domain functions $p(t)$,$q(t)$ is defined as

$$\mathcal{X}_{p,q}(\tau, \nu) \coloneqq \int p(t)q^*(t-\tau)e^{-j2\pi\nu(t-\tau)}dt \quad (43)$$

- The cross-ambiguity function of two frequency domain functions $P(f)$,$Q(f)$ is defined as

$$\mathcal{Y}_{P,Q}(\tau, \nu) \coloneqq \int P(f)Q^*(f-\nu)e^{j2\pi\tau f}df \quad (44)$$

Note that $\mathcal{X}_{p,q}(\tau, \nu) = \mathcal{Y}_{P,Q}(\tau, \nu)$ if $P(f)$ is the Fourier transform of $p(t)$ and $Q(f)$ is the Fourier transform of $q(t)$. For the sake of brevity, we also define $\mathcal{X}_p(\tau, \nu) \coloneqq \mathcal{X}_{p,p}(\tau, \nu)$ and $\mathcal{Y}_P(\tau, \nu) \coloneqq \mathcal{Y}_{P,P}(\tau, \nu)$ to represent the auto-ambiguity functions.

Definition 8: The auto-correlation functions $\mathcal{R}_p(\tau)$, $\mathcal{R}_Q(\nu)$ of $p(t)$ and $Q(f)$ respectively are defined as

$$\mathcal{R}_p(\tau) \coloneqq \int p(t)p^*(t-\tau)dt \quad (45)$$

$$\mathcal{R}_Q(\nu) \coloneqq \int Q(f)Q^*(f-\nu)df \quad (46)$$

We begin by considering a Type-1 TC filter $g(\tau, \nu) = \alpha(\tau)\beta(\nu)$. By evaluating the twisted convolution, it can be shown that

$$g *_\sigma g^\dagger(\tau, \nu) = \mathcal{X}_\alpha(\tau, \nu)\mathcal{R}_\beta(\nu). \quad (47)$$

Hence from Theorem 3, the noise covariance function is

$$C_{\mathcal{Z}_{n^g}}(\tau_l, \nu_k|\tau_{l'}, \nu_{k'}) = \sum_{(m,n)\in\mathbb{Z}^2} \mathcal{X}_\alpha(\tau_l - \tau_{l'} - nT, \nu_k - \nu_{k'} - m\Delta f)\ \mathcal{R}_\beta(\nu_k - \nu_{k'} - m\Delta f)\ e^{j2\pi\nu_k nT}e^{j2\pi\tau_{l'}(\nu_k-\nu_{k'}-m\Delta f)}$$

Suppose that $\beta(\nu)$ is a square root Nyquist pulse with sampling interval $\frac{\Delta f}{N}$. Then $\mathcal{R}_\beta(\nu_k - \nu_{k'} - m\Delta f) = \delta[k - k' - mN]$. In this case,

$$C_{\mathcal{Z}_{n^g}}(\tau_l, \nu_k|\tau_{l'}, \nu_{k'}) = \sum_{(m,n)\in\mathbb{Z}^2} \mathcal{X}_\alpha(\tau_l - \tau_{l'} - nT, 0)\delta\big[k - k' - mN\big]e^{j2\pi\frac{nk}{N}}.$$

Note that $\mathcal{X}_\alpha(\tau_l - \tau_{l'} - nT, 0) = \mathcal{R}_\alpha(\tau_l - \tau_{l'} - nT)$. Now suppose that $\alpha(\tau)$ is also a square root Nyquist pulse, with sampling interval $\frac{T}{M}$. Then $\mathcal{R}_\alpha(\tau_l-\tau_{l'}-nT) = \delta[l-l'-nM]$. Hence we obtain

$$C_{\mathcal{Z}_{n^g}}(\tau_l, \nu_k|\tau_{l'}, \nu_{k'}) = \sum_{(m,n)\in\mathbb{Z}^2} \delta\big[l - l' - nM\big]\delta\big[k - k' - mN\big]e^{j2\pi\frac{nk}{N}}. \quad (48)$$

This means that the noise samples $\{n_{\mathrm{dd}}[l, k]\}$ for $(l, k) \in \{0, \ldots, M-1\} \times \{0, \ldots, N-1\}$ are uncorrelated.

For a Type-2 TC filter, $g(\tau, \nu) = \alpha(\tau)\beta(\nu)e^{j2\pi\nu\tau}$, note that $g *_\sigma g^\dagger(\tau, \nu) = \mathcal{R}_\alpha(\tau)\mathcal{Y}_\beta(\tau, \nu)$, and hence the same result can be obtained for square root Nyquist pulses. We summarize this key result on Type-1 and Type-2 TC filters with square root Nyquist pulses as the following theorem.

Theorem 4: For receive TC filter $g^{Rx}(\tau, \nu)$ that is either Type-1 or Type-2, the output noise samples $n_{dd}[l, k]$ for $(l, k) \in \{0, \ldots, M-1\} \times \{0, \ldots, N-1\}$ are uncorrelated, if both the following conditions hold.

- $A(f)$ is a square root Nyquist window, *i.e.,* $|A(f)|^2$ is a Nyquist window, or equivalently $\alpha(\tau)$ is a square root Nyquist pulse with sampling interval $\frac{T}{M}$.
- $B(t)$ is a square root Nyquist window, *i.e.,* $|B(t)|^2$ is a Nyquist window, or equivalently $\beta(\nu)$ is a square root Nyquist pulse with sampling interval $\frac{\Delta f}{N}$.

Remark 5: For a Type-1 or a Type-2 receive TC filter, we note that the receive pulses $\psi^{\tilde{g}^{\mathrm{Rx}}}_{l,k}(t)$ for $(l, k) \in \{0, \ldots, M-1\} \times \{0, \ldots, N-1\}$ form an orthogonal set when using square root Nyquist windows. This is the underlying reason for uncorrelated noise samples in Theorem 4.

C. DD DOMAIN INPUT-OUTPUT RELATIONSHIP FOR TC FILTERED WHITE GAUSSIAN NOISE

We now use Theorem 3 and Type-1 sinc TC filters to define a DD domain representation $\mathcal{Z}_n(\tau, \nu)$ for the white noise $n(t)$ as a Gaussian process. We will use this to present a DD domain input-output relationship for TC filtered white noise processes.

Consider a sequence of TC filters $g_{M',N'}(\tau, \nu) \coloneqq 2M'\Delta f\mathrm{sinc}(2M'\Delta f\tau)\ 2N'T\mathrm{sinc}(2N'T\nu)$ where the scale parameters $(M', N') \in \mathbb{R}^2_+$. Note that this Type-1 TC filter

corresponds to windowing by a rectangular time window with support $[-N'T, N'T]$ followed by windowing by a rectangular frequency window with support $[-M'\Delta f, M'\Delta f]$. The true white noise process can therefore be imagined as the limiting TC filtered noise process by taking $N' \to \infty$ first, followed by taking $M' \to \infty$.

By Theorem 3, the $(M', N')^{\text{th}}$ TC filtered noise process $\mathcal{Z}_{n^{g_{M',N'}}}(\tau, \nu)$ is a zero mean Gaussian noise process where the covariance function depends on $g_{M',N'} *_\sigma g^\dagger_{M',N'}(\tau, \nu)$. By evaluating (47) for $\alpha(\tau) = 2M'\Delta f \text{sinc}(2M'\Delta f\tau)$ and $\beta(\nu) = 2N'T\text{sinc}(2N'T\nu)$ (using (65) from [8]), we note that

$$g_{M',N'} *_\sigma g^\dagger_{M',N'}(\tau, \nu) = 2N'T\text{sinc}\big(2N'T\nu\big)e^{j\pi\tau\nu}$$
$$2M'\Delta f\left(1 - \frac{|\nu|}{2M'\Delta f}\right)\text{sinc}\big(\tau(2M'\Delta f - |\nu|)\big) \tag{49}$$

By taking $N' \to \infty$, $2N'T\text{sinc}(2N'T\nu) \to \delta(\nu)$ and hence

$$\lim_{N'\to\infty} g_{M',N'} *_\sigma g^\dagger_{M',N'}(\tau, \nu) = \delta(\nu)2M'\Delta f\text{sinc}\big(2M'\Delta f\tau\big)$$

Now by taking $M' \to \infty$, we get

$$\lim_{M'\to\infty}\lim_{N'\to\infty} g_{M',N'} *_\sigma g^\dagger_{M',N'}(\tau, \nu) = \delta(\nu)\delta(\tau) \tag{50}$$

Hence by Theorem 3, we can treat white noise in the DD domain as the limiting process, which is a zero mean non-stationary Gaussian noise process with the covariance function $C_{\mathcal{Z}_n}(\tau, \nu|\tau', \nu')$ given as follows:

$$C_{\mathcal{Z}_n}\big(\tau, \nu|\tau', \nu'\big) = \frac{N_0}{T}\sum_{(m,n)\in\mathbb{Z}^2} e^{j2\pi\nu' nT}\delta\big(\tau - \tau' - nT\big)$$
$$\delta\big(\nu - \nu' - m\Delta f\big). \tag{51}$$

Using (51) and Theorem 3, we can now establish the following DD domain input-output relationship for TC filtered white noise, as follows:

$$\mathcal{Z}_{n^g}(\tau, \nu) = g *_\sigma \mathcal{Z}_n(\tau, \nu). \tag{52}$$

Remark 6: This twisted convolution input-output relationship (52) demonstrates that when a white Gaussian process is TC filtered, the output in the DD domain is a zero mean Gaussian processes with covariance function:

$$C_{\mathcal{Z}^g_n}\big(\tau, \nu|\tau', \nu'\big) = g *_\sigma g^\dagger *_\sigma C_{\mathcal{Z}_n}\big(\tau, \nu|\tau', \nu'\big) \tag{53}$$

where $C_{\mathcal{Z}_n}(\tau, \nu|\tau', \nu')$ is the covariance function of the input white noise.

V. OPTIMAL ZAK-OTFS RECEIVER FOR DOUBLY DISPERSIVE CHANNELS

In this section, we provide the characterization of the optimal Zak-OTFS receiver for doubly dispersive channels, where the optimal receiver is defined as follows.

Definition 9: An optimal Zak-OTFS receiver is the one whose output symbols $y_{dd}[l, k]$ are sufficient statistics for maximum likelihood (ML) detection of the input data symbols $(\hat{x}[l, k])$.

We will show that the optimal receive TC filter is the one that is matched to the twisted convolution of the channel DD response with the transmit TC filter, and that DD sampling on the grid with this optimal receive TC filter provides the sufficient statistics for ML detection.

Consider a doubly dispersive channel with DD response $h(\tau, \nu)$ as in (5)-(6). The received signal $y(t) = h *_\sigma x(t) + n(t)$ can be expressed as

$$y(t) = \sum_{l=0}^{M-1}\sum_{k=0}^{N-1} \hat{x}[l, k]\phi^{h*_\sigma g^{\text{Tx}}}_{\tau_l,\nu_k}(t) + n(t) \tag{54}$$

Let $\hat{\boldsymbol{x}} := (\hat{x}[l, k])$ denote the transmit symbol vector. Following similarly as in [15, Sec. 9.3-1], the optimal $\hat{\boldsymbol{x}}_{\text{opt}}$ that has the smallest probability of symbol error is the ML estimate $\hat{\boldsymbol{x}}_{\text{est}}$ that minimizes $\int |y(t) - \sum_{l=0}^{M-1}\sum_{k=0}^{N-1} \hat{x}_{\text{est}}[l, k]\phi^{h*_\sigma g^{\text{Tx}}}_{\tau_l,\nu_k}(t)|^2 dt$. Hence, the ML estimate $\hat{\boldsymbol{x}}_{\text{opt}}$ is the $\hat{\boldsymbol{x}}_{\text{est}}$ that maximizes

$$2\text{Re}\left(\sum_{l,k}\hat{x}^*_{\text{est}}[l, k]\int y(t)\Big(\phi^{h*_\sigma g^{\text{Tx}}}_{\tau_l,\nu_k}(t)\Big)^* dt\right)$$
$$-\sum_{l,k}\sum_{l',k'}\hat{x}^*_{\text{est}}[l, k]\hat{x}_{\text{est}}\big[l', k'\big]\int\Big(\phi^{h*_\sigma g^{\text{Tx}}}_{\tau_l,\nu_k}(t)\Big)^*\phi^{h*_\sigma g^{\text{Tx}}}_{\tau_{l'},\nu_{k'}}(t)dt.$$

where $\text{Re}(\cdot)$ represent the real part of a complex number.

Hence, $y^{\text{opt}}[l, k] := \int y(t)(\phi^{h*_\sigma g^{\text{Tx}}}_{\tau_l,\nu_k}(t))^* dt$ are sufficient statistics for ML detection. The optimal receiver that recovers $y^{\text{opt}}[l, k]$ is presented in the following theorem.

Theorem 5: For a doubly dispersive channel with response $h(\tau, \nu)$, the optimal Zak-OTFS receiver is as follows:

- The optimal Zak-OTFS receive TC filter is $g^{Rx}(\tau, \nu) = (h *_\sigma g^{Tx}(\tau, \nu))^\dagger$ which is matched to the cascade $h *_\sigma g^{Tx}(\tau, \nu)$ of the transmit TC filter and the channel.
- The output symbols $y_{dd}[l, k] = \mathcal{Z}_{y^{g^{Rx}}}(\tau_l, \nu_k)$ obtained by sampling the optimal TC filtered received signal on the DD grid points are sufficient statistics for ML detection of input data symbols $\hat{\boldsymbol{x}}$.

Proof: See Appendix C. ∎

With regard to implementation, note that the optimal receive TC filter depends on the channel realization of $h(\tau, \nu)$. For a general channel response, $h(\tau, \nu)$, the matched TC filter might not have a Type-1 or Type-2 structure, which means it is not possible to implement the matched TC filter using time and frequency windowing techniques. Furthermore, knowledge of the DD channel response $h(\tau, \nu)$ is also required, which is impractical when the channel response $h(\tau, \nu)$ is continuous and non-sparse.

In the paper, we hence focus on the optimal TC filter for the practical case of a sparse doubly dispersive channel with P paths, where $h(\tau, \nu) = \sum_{p=0}^{P-1} h_p\delta(\tau - \tau_{l_p})\delta(\nu - \nu_{k_p})$. We will discuss the implementation of the optimal TC filter. We will show that it is sufficient to match the receive TC filter to the transmit TC filter under certain conditions referred to as the crystalline regime conditions. We will first introduce the concepts of effective channel response and crystalline regime for Type-1 and Type-2 Zak-OTFS implementations that are required for the discussion.

VI. EFFECTIVE CHANNEL RESPONSE OF TYPE-1 AND TYPE-2 ZAK-OTFS IMPLEMENTATIONS

In this section, we present the effective channel response of Type-1 and Type-2 Zak-OTFS implementations for a given choice of transmit and receive windows (or equivalently TC filters). Recall that a Type-1 implementation uses a Type-1 transmit TC filter and the matched Type-2 receive TC filter, whereas a Type-2 implementation uses a Type-2 transmit TC filter and the matched Type-1 receive TC filter.

We show that the effective channel response depends on the ambiguity functions of the windows. We then introduce the crystalline regime conditions for Type-1 and Type-2 Zak-OTFS implementations. In the crystalline regime, we establish the convergence of ambiguity functions to corresponding auto-correlation functions, when the channel spread is smaller than DD grid dimensions $(T, \Delta f)$. This means the effective channel response in the crystalline regime depends on the auto-correlation functions. In the next section, we use these results to derive the structure of the optimal Zak-OTFS receiver implementation.

We will show that the DD domain effective channel response depends on the cross-ambiguity functions of the transmit and the receive windows. First, we introduce the necessary notation and definitions. Let the frequency windows at the transmitter and the receiver be $A^{\mathrm{Tx}}(f)$ and $A^{\mathrm{Rx}}(f)$ respectively. Similarly let the time windows at the transmitter and the receiver be $B^{\mathrm{Tx}}(t)$ and $B^{\mathrm{Rx}}(t)$ respectively. As such, $\alpha^{\mathrm{Tx}}(\tau)$, $\beta^{\mathrm{Tx}}(\nu)$ and $\alpha^{\mathrm{Rx}}(\tau)$, $\beta^{\mathrm{Rx}}(\nu)$ are the delay and the Doppler components of the TC filters at the transmitter and the receiver respectively.

The following theorem presents the effective DD channel characterizations for Type-1 and Type-2 Zak-OTFS implementations. It can be noted the effective channel is linked to the ambiguity functions of the transmit and receive windows.

Theorem 6: For a Type-1 Zak-OTFS implementation, the effective channel response is

$$h_{dd}(\tau,\nu) = \iint h(\tau',\nu') e^{j2\pi(\nu\tau-\nu'\tau')} \mathcal{Y}_{A^{Tx},(A^{Rx})^*}(\tau-\tau',-\nu') \mathcal{X}_{B^{Tx},(B^{Rx})^*}(-\tau,\nu-\nu') d\tau' d\nu' \tag{55}$$

For a Type-2 Zak-OTFS implementation, the effective channel response is

$$h_{dd}(\tau,\nu) = \iint h(\tau',\nu') e^{j2\pi(\nu\tau-\nu'\tau')} \mathcal{Y}_{A^{Tx},(A^{Rx})^*}(\tau-\tau',-\nu) \mathcal{X}_{B^{Tx},(B^{Rx})^*}(-\tau',\nu-\nu') d\tau' d\nu' \tag{56}$$

Proof: See Appendix D. ∎

Our focus is on the case where the TC filter at the receiver is matched to the TC filter at the transmitter. Hence as mentioned earlier, we consider the following case: $A^{\mathrm{Tx}}(f) = A(f), A^{\mathrm{Rx}}(f) = A^*(f)$ and $B^{\mathrm{Tx}}(t) = B(t), B^{\mathrm{Rx}}(t) = B^*(t)$. In this case, $\mathcal{Y}_{A^{\mathrm{Tx}},(A^{\mathrm{Rx}})^*}(\tau,\nu)$ equals the auto ambiguity function $\mathcal{Y}_A(\tau,\nu)$, and $\mathcal{X}_{B^{\mathrm{Tx}},(B^{\mathrm{Rx}})^*}(\tau,\nu)$ equals the auto ambiguity function $\mathcal{X}_B(\tau,\nu)$.

For a sparse channel with P paths, the channel response $h(\tau,\nu) = \sum_{p=0}^{P-1} h_p \delta(\tau-\tau_{l_p})\delta(\nu-\nu_{k_p})$. From Theorem 6, the effective channel response for a Type-1 implementation is given by

$$h^{(1)}_{\mathrm{dd}}(\tau,\nu) = \sum_{p=0}^{P-1} h_p e^{j2\pi\left(\nu\tau-\nu_{k_p}\tau_{l_p}\right)} \mathcal{Y}_A\left(\tau-\tau_{l_p},-\nu_{k_p}\right) \mathcal{X}_B\left(-\tau,\nu-\nu_{k_p}\right) \tag{57}$$

whereas for a Type-2 implementation, it is given by

$$h^{(2)}_{\mathrm{dd}}(\tau,\nu) = \sum_{p=0}^{P-1} h_p e^{j2\pi\left(\nu\tau-\nu_{k_p}\tau_{l_p}\right)} \mathcal{Y}_A\left(\tau-\tau_{l_p},-\nu\right) \mathcal{X}_B\left(-\tau_{l_p},\nu-\nu_{k_p}\right) \tag{58}$$

Consider the following rectangular windows $A(f) = \frac{1}{\sqrt{M\Delta f}}\mathbb{I}_{[0,M\Delta f)}(f)$ and $B(t) = \frac{1}{\sqrt{NT}}\mathbb{I}_{[0,NT)}(t)$ where $\mathbb{I}_S(a)$ is the indicator function, which equals 1 if $a \in S$ and 0 otherwise. Figure 3 illustrates the effective channel response of a two path channel for $M = 4, N = 4$, where the red dotted rectangle is of dimensions $T \times \Delta f$. It can be noted that the effective channel response is not localized within this rectangle.

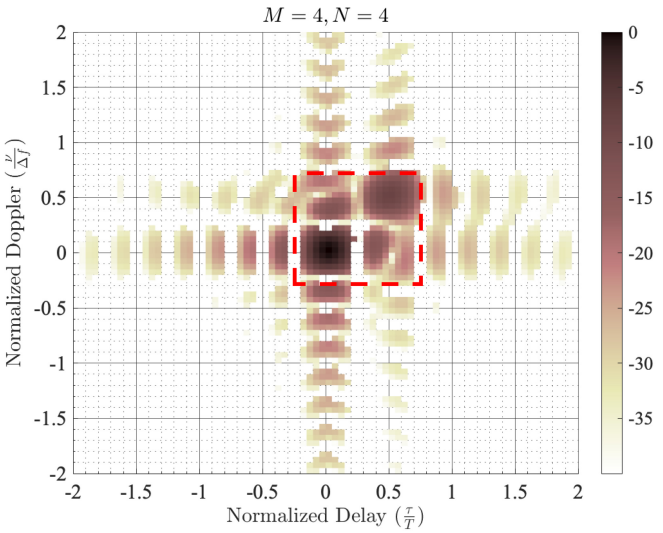

FIGURE 3. Plot of the effective channel gain $|h_{\mathrm{dd}}(\tau,\nu)|$ (in dB) for rectangular windows with $M = 4$, $N = 4$.

A. CRYSTALLINE REGIME

The concept of *crystalline regime* was first defined in [8]. It is the regime where the effective channel response is compact and is localized (in the sense of having most of its energy) in a fundamental rectangular region of dimensions $T \times \Delta f$ [8], and hence there is negligible effect of DD domain aliasing. Crystalline regime is crucial for Zak-OTFS channel predictability performance which deals with accuracy of measured effective channel taps [8], [9].

Figure 4 shows an illustration of the channel response for rectangular windows with $(M, N) = (32, 32)$. As can be observed, now the spread of the effective channel is much smaller, and is almost localized within a fundamental

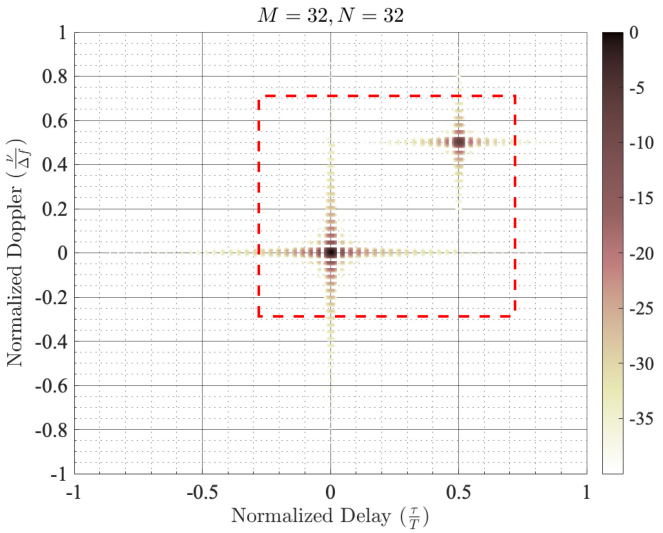

FIGURE 4. Plot of the effective channel gain $|h_{\text{dd}}(\tau, \nu)|$ (in dB) for rectangular windows with $M = 32$, $N = 32$.

rectangular region depicted in red. This demonstrates that as the window supports get larger, the effective channel response becomes more localized around the path DD locations. Hence, large window supports are a necessary feature of the crystalline regime.

Let W_A denote the support of the frequency window $A(f)$ and W_B denote the support of the time window $B(t)$.[5]

Remark 7: For the crystalline regime condition to hold, it is required that

$$W_A \gg \Delta f; W_B \gg T \tag{59}$$

as well as $\Delta f > \nu_{\max}$, the Doppler spread, and $T > \tau_{\max}$, the delay spread.

To derive results for the crystalline regime, we restrict to the class of windows that have square integrable auto-correlation functions, and the auto-correlation functions are Lipschitz continuous on the positive real line. Note that this allows for a wide range of functions, including rectangular and root-raised cosine (RRC) windows.

Lemma 1: Consider a family of window functions $\{A_W(f)\}_{W \geq 1}$ formed from a prototype unit window $A_1(f)$ that has unit support. $A_W(f) := \sqrt{\frac{1}{W}} A_1(\frac{f}{W})$ is the scaled window that has support W with the same energy and shape as $A_1(f)$. Suppose that the auto-correlation function $\mathcal{R}_{A_1}(\nu)$ is Lipschitz continuous on $[0, \infty)$. Then $\exists K_{A_1} > 0$ such that

$$\left|\mathcal{Y}_{A_W}(\tau, \nu) - \mathcal{R}_{\alpha_W}(\tau)\right| \leq K_{A_1} \sqrt{\frac{|\nu|}{W}}$$

for all $(\tau, \nu) \in \mathbb{R}^2$.

[5]For general windows that are not finitely supported, our results can be extended by considering the variances $\int t^2 |B(t)|^2 dt$ (and $\int f^2 |A(f)|^2 df$) to be much larger compared to the fundamental periods T (and Δf) respectively. We use window supports in the paper, since in engineering applications, other notions of support, such as half-power bandwidth and first-null bandwidth, are typically used for non-finite support windows.

Proof: See Appendix D. ■

Lemma 1 shows that the ambiguity function $\mathcal{Y}_{A_W}(\tau, \nu)$ converges to $\mathcal{R}_{\alpha_W}(\tau)$ uniformly, as $\frac{|\nu|}{W} \to 0$, *i.e.,* for Doppler shifts ν that are significantly smaller than the frequency window support W.

Note 3: An identical result to Lemma 1 can be obtained for time domain windows that have Lipschitz continuous correlation functions. Hence, we take the following results (60)-(61) to hold for the Zak-OTFS window functions $A(f), B(t)$ considered in the paper.

$$\mathcal{Y}_A(\tau, \nu) = \mathcal{R}_\alpha(\tau) + O\left(\sqrt{\frac{|\nu|}{W_A}}\right) \tag{60}$$

$$\mathcal{X}_B(\tau, \nu) = \mathcal{R}_\beta(\nu) + O\left(\sqrt{\frac{|\tau|}{W_B}}\right) \tag{61}$$

By applying (60)-(61), we will now show that the effective channel response depends on the auto-correlation functions of the delay shape $\alpha(\tau)$ and Doppler shape $\beta(\nu)$, when operating in the crystalline regime. Note that since $\mathcal{R}_\alpha(\tau)$ is the auto-correlation function of $\alpha(t)$, it is also the inverse Fourier transform of $|A(f)|^2$. This means that the resulting effective pulse shape along the delay axis is the inverse Fourier transform of the product of the transmit window $A(f)$ and the receive window $A^*(f)$. Similarly, $\mathcal{R}_\beta(\nu)$ is the Fourier transform of $|B(t)|^2$.

Consider the effective channel response for a Type-1 implementation given in (57). In the crystalline regime, note from (60) that $\mathcal{Y}_A(\tau - \tau_{l_p}, -\nu_{k_p}) \approx \mathcal{R}_\alpha(\tau - \tau_{l_p})$, since $W_A \gg \Delta f > |\nu_{k_p}|$ from Remark 7. Also since $T \gg \frac{1}{w_A}$, $\mathcal{R}_\alpha(\tau - \tau_{l_p})$ is localized (in the sense of having almost all its energy) in a small interval of length $2T'$, $[\tau_{l_p} - T', \tau_{l_p} + T']$, such that $2T' + \tau_{\max} < T$. As a result, $\mathcal{R}_\alpha(\tau - \tau_{l_p}) \approx 0$ for $|\tau| \geq T$. For $|\tau| \leq T$, note that $\mathcal{X}_B(-\tau, \nu - \nu_{k_p}) \approx \mathcal{R}_\beta(\nu - \nu_{k_p})$ from (61), since $W_B \gg T$ from Remark 7. Let $w_B := \frac{W_B}{T}$ and $w_A := \frac{W_A}{\Delta f}$; then more formally,

$$\lim_{w_B \uparrow \infty} \lim_{w_A \uparrow \infty} \mathcal{Y}_A(\tau - \tau_{l_p}, -\nu_{k_p}) \mathcal{X}_B(-\tau, \nu - \nu_{k_p}) = \mathcal{R}_\alpha(\tau - \tau_{l_p}) \mathcal{R}_\beta(\nu - \nu_{k_p})$$

for each τ, ν.

Hence, for a Type-1 implementation, the effective channel response in the crystalline regime is given by

$$\bar{h}_{\text{dd}}(\tau, \nu) = \sum_{p=0}^{P-1} h_p e^{j2\pi\left(\nu\tau - \nu_{k_p}\tau_{l_p}\right)} \mathcal{R}_\alpha(\tau - \tau_{l_p}) \mathcal{R}_\beta(\nu - \nu_{k_p}) \tag{62}$$

We summarize the crystalline approximation result for a general channel $h(\tau, \nu)$ as a corollary of Theorem 6 as follows:

Corollary 3: For either a Type-1 Zak-OTFS implementation or a Type-2 Zak-OTFS implementation, the effective channel response in the crystalline regime is given by

$$\left(g^{Tx}\right)^{\dagger} *_{\sigma} h *_{\sigma} g^{Tx}(\tau, \nu) \approx \bar{h}_{dd}(\tau, \nu) \tag{63}$$

$$:= \iint h(\tau', \nu') e^{j2\pi(\nu\tau - \nu'\tau')} \mathcal{R}_{\alpha}(\tau - \tau') \mathcal{R}_{\beta}(\nu - \nu') d\tau' d\nu'$$

$$= e^{j2\pi\nu\tau} \left(h(\tau, \nu) e^{-j2\pi\nu\tau} \star \left(\mathcal{R}_{\alpha}(\tau) \mathcal{R}_{\beta}(\nu) \right) \right) \tag{64}$$

where $\star$ denotes 2D convolution.

We have presented our results for the matched TC filter case, however, they can be applied for more general Type-1 and Type-2 TC filters as follows. The effective DD domain pulse shape along the delay axis is the inverse Fourier transform of $A^{\mathrm{Tx}}(f)A^{\mathrm{Rx}}(f)$, where as the pulse shape along Doppler axis is the Fourier transform of $B^{\mathrm{Tx}}(t)B^{\mathrm{Rx}}(t)$, in the crystalline regime.

VII. RADAR MATCHED FILTER WITH PULSONES VS. TYPE-1 AND TYPE-2 ZAK-OTFS

In this section, we compare a Type-1 and Type-2 Zak-OTFS receiver with the traditional radar matched filter (which is optimal) in a single target radar scenario. We show that in the crystalline regime, the performance gap is negligible in terms of SNR, delay resolution and Doppler resolution. This result highlights the suitability of Zak-OTFS waveform for integrated sensing and communication.

We also show that the optimal Zak-OTFS receiver for a single reflector channel is closely linked to radar matched filter processing. We use the insights derived here for implementation of the optimal Zak-OTFS receiver for sparse doubly dispersive channels.

Consider a single reflector channel as follows:

$$y(t) = s(t - \tau_{\circ}) e^{j2\pi\nu_{\circ}(t-\tau_{\circ})} + n(t) \tag{65}$$

where $s(t)$ is the transmitted signal, $y(t)$ is the received signal and $n(t)$ is an additive white Gaussian noise (AWGN) process with power spectral density N_0 Watts per Hz. We note that $(\tau_{\circ}, \nu_{\circ}) \in [0, T) \times [-\Delta f/2, \Delta f/2)$.

A. OPTIMAL ZAK-OTFS RECEIVER FOR SINGLE REFLECTOR CHANNEL

Note that for this channel, the Zak-OTFS correlating receive pulse $\psi^{\tilde{g}^{\mathrm{Rx}}}_{\tau_l,\nu_k}(t)$ corresponding to the output sample at (τ_l, ν_k) (using the optimal receive TC filter $g^{\mathrm{Rx}}(\tau, \nu) = (h *_{\sigma} g^{\mathrm{Tx}}(\tau, \nu))^{\dagger}$) is

$$\psi^{\tilde{g}^{\mathrm{Rx}}}_{\tau_l,\nu_k}(t) = \frac{1}{T} \left(h *_{\sigma} \phi^{g^{\mathrm{Tx}}}_{\tau_l,\nu_k}(t) \right)^* \tag{66}$$

$$= \frac{1}{T} \left(\phi^{g^{\mathrm{Tx}}}_{\tau_l,\nu_k}(t - \tau_{\circ}) \right)^* e^{-j2\pi\nu_{\circ}(t-\tau_{\circ})}. \tag{67}$$

since $h(\tau, \nu) = \delta(\tau - \tau_{\circ})\delta(\nu - \nu_{\circ})$.

Hence by Theorem 1, the Zak-OTFS output $y_{\mathrm{dd}}[l, k] = \mathcal{Z}_{y g^{\mathrm{Rx}}}(\tau_l, \nu_k)$ corresponding to the optimal receive TC filter $g^{\mathrm{Rx}}(\tau, \nu) = (h *_{\sigma} g^{\mathrm{Tx}}(\tau, \nu))^{\dagger}$ is

$$\mathcal{Z}_{y g^{\mathrm{Rx}}}(\tau_l, \nu_k) = \int y(t) \psi^{\tilde{g}^{\mathrm{Rx}}}_{\tau_l,\nu_k}(t) dt = \frac{1}{T} \mathcal{X}_{y,\phi^{g^{\mathrm{Tx}}}_{\tau_l,\nu_k}}(\tau_{\circ}, \nu_{\circ}). \tag{68}$$

We will now show that this optimal receiver is closely related to the traditional radar matched filter approach in this channel.

B. RADAR MATCHED FILTER IN SINGLE TARGET CHANNEL

In the radar context, the channel in (65) is a single target channel with the target at DD location $(\tau_{\circ}, \nu_{\circ})$, and $s(t)$ is the input radar pulse. The traditional radar approach [8] to estimate the target's delay and Doppler shift, is to obtain the maximum likelihood estimate as

$$\left(\hat{\tau}, \hat{\nu}\right) := \arg \max_{(\tau,\nu)\in\mathcal{S}} \left| \mathcal{X}_{y,s}(\tau, \nu) \right| \tag{69}$$

where $\mathcal{S} \subseteq [0, T) \times [-\Delta f/2, \Delta f/2)$ is the region of interest. The estimation process requires evaluating the samples of the ambiguity function $\mathcal{X}_{y,s}(\tau, \nu)$ to find its peak.

Let the signal component of the received signal $y(t)$ be $r(t) := s(t - \tau_{\circ})e^{j2\pi\nu_{\circ}(t-\tau_{\circ})}$. Let $r_{\tau,\nu}$ denote the signal component of the ambiguity function sample $\mathcal{X}_{y,s}(\tau, \nu)$ at the point (τ, ν) as

$$r_{\tau,\nu} := \mathcal{X}_{r,s}(\tau, \nu) \tag{70}$$

$$= e^{j2\pi\nu_{\circ}(\tau-\tau_{\circ})} \mathcal{X}_{s,s}(\tau - \tau_{\circ}, \nu - \nu_{\circ}) \tag{71}$$

and let $n_{\tau,\nu} := \mathcal{X}_{n,s}(\tau, \nu)$ be the noise component. Let $\sigma^2_{\tau,\nu} := \mathbb{E}[|n_{\tau,\nu}|^2]$ denote the noise variance. Hence the SNR at sample point (τ, ν) is

$$\frac{|r_{\tau,\nu}|^2}{\sigma^2_{\tau,\nu}} = \frac{\left|\mathcal{X}_{s,s}(\tau - \tau_{\circ}, \nu - \nu_{\circ})\right|^2}{N_0 \mathcal{X}_{s,s}(0, 0)} \tag{72}$$

The signal-to-noise ratio (SNR) $\frac{|r_{\tau,\nu}|^2}{\sigma^2_{\tau,\nu}}$ is maximized at the target location $(\tau, \nu) = (\tau_{\circ}, \nu_{\circ})$. Note that sampling the ambiguity function $\mathcal{X}_{y,s}(\tau, \nu)$ at (τ', ν') is equivalent to correlation of the received signal $y(t)$ with the pulse $s^*(t - \tau')e^{-j2\pi\nu'(t-\tau')}$. Hence, the radar matched filter approach is correlating the received signal $y(t)$ with the pulse $s^*(t - \tau_{\circ})e^{-j2\pi\nu_{\circ}(t-\tau_{\circ})}$ corresponding to the target location $(\tau_{\circ}, \nu_{\circ})$.

Remark 8: Hence from (68), for a single reflector channel, the Zak-OTFS output $y_{dd}[l, k]$ corresponding to the optimal receive TC filter $(h *_{\sigma} g^{Tx}(\tau, \nu))^{\dagger}$ can be obtained using radar matched filter processing of the received signal $y(t)$, treating $\phi^{g^{Tx}}_{\tau_l,\nu_k}(t)$ as the input radar pulse $s(t)$. Under such an implementation, the radar matched filter output sampled at location $(\tau_{\circ}, \nu_{\circ})$ yields $Ty_{dd}[l, k]$.

Note that this optimal Zak-OTFS receiver implementation is not a standard radar implementation where an ambiguity function (obtained with respect to a single radar prototype pulse) is sampled. In contrast, the approach here requires computation of one sample from each of the MN ambiguity functions in (68), which is potentially highly complex. Moreover, it clearly cannot be implemented directly using a standard Type-1 and Type-2 Zak-OTFS receiver approach of a time and frequency windowing block followed by a DZT block as in Figure 1.

In the next two subsections, we will focus on the radar sensing problem in the single target channel using a Zak-OTFS pulsone as a radar pulse. We will show that the SNR curves obtained from a radar matched filter implementation and a Type-1 (or a Type-2) Zak-OTFS implementation

TABLE 2. The two approaches for a single target radar channel with the transmit radar pulse $\phi^{g^{\mathrm{Tx}}}_{\tau_l,\nu_k}(t)$.

Receiver Approach	Output for (τ,ν)
Radar Matched Filter	$\mathcal{X}_{y,\phi^{g^{\mathrm{Tx}}}_{\tau_l,\nu_k}}(\tau,\nu)$
Type-1 and Type-2 Zak-OTFS	$(g^{\mathrm{Tx}})^{\dagger} *_{\sigma} \mathcal{Z}_y(\tau_l+\tau,\nu_k+\nu)$

are the same in the crystalline regime. We will use the insights derived here to present a time-frequency windowing based implementation of the optimal Zak-OTFS receiver for general sparse doubly dispersive channels.

The processing outputs of the two approaches are summarized in Table 2. As noted here, the radar approach output is the ambiguity function sample of the received signal $y(t)$ computed with respect to the input radar pulse $\phi^{g^{\mathrm{Tx}}}_{\tau_l,\nu_k}(t)$, whereas the Type-1 and Type-2 Zak-OTFS output is the DD domain sample of the TC filtered received signal (matched to the transmitter $g^{\mathrm{Tx}}(\tau,\nu)$) and sampled at $(\tau_l+\tau,\nu_k+\nu)$.

C. RADAR MATCHED FILTER WITH ZAK-OTFS PULSONES

Let the transmitted radar signal $s(t)$ be the Type-1 Zak-OTFS pulsone $\phi^{g_1}_{\tau_l,\nu_k}(t)$, *i.e.,* Type-1 Zak-OTFS transmit pulse. Note that in this case, the signal component of the radar matched filter output can be evaluated as

$$\begin{aligned}&\mathcal{X}_{s,s}(\tau-\tau_\circ,\nu-\nu_\circ)\\&=T\sum_{(m,n)\in\mathbb{Z}^2}\mathcal{Y}_A(\tau-\tau_\circ+nT,\nu-\nu_\circ)\\&\qquad\mathcal{X}_B(-nT,\nu-\nu_\circ+m\Delta f)\;e^{-j2\pi\nu_k nT}e^{j2\pi m\Delta f\tau_l}\end{aligned}\tag{73}$$

In the crystalline regime, since $|\nu-\nu_\circ|<\Delta f\ll W_A$, recall that $\mathcal{Y}_A(\tau-\tau_\circ+nT,\nu-\nu_\circ)\approx R_\alpha(\tau-\tau_\circ+nT)$ by (60). Also recall that $R_\alpha(\tau')\approx 0,\forall\tau':|\tau'|\geq T$ since it is localized in a very small region $[-T',T']$ where $T'<T$. Hence, $R_\alpha(\tau-\tau_\circ+nT)\approx 0,\ \forall n:|n|>1$ (since $\tau-\tau_\circ\in[-T,T]$). Hence, we obtain the radar ambiguity function as

$$\begin{aligned}\mathcal{X}_{s,s}(\tau-\tau_\circ,\nu-\nu_\circ)\approx T\sum_{n=-1}^{1}\mathcal{R}_\alpha(\tau-\tau_\circ+nT)e^{-j2\pi\nu_k nT}\\\sum_{m\in\mathbb{Z}}\mathcal{X}_B(-nT,\nu-\nu_\circ+m\Delta f)\;e^{j2\pi m\Delta f\tau_l}\end{aligned}$$

Repeating the same arguments for time window $B(t)$, the crystalline regime ambiguity function can be obtained as

$$\begin{aligned}\mathcal{X}_{s,s}(\tau-\tau_\circ,\nu-\nu_\circ)\approx T\sum_{n=-1}^{1}\mathcal{R}_\alpha(\tau-\tau_\circ+nT)e^{-j2\pi\nu_k nT}\\\sum_{m=-1}^{1}\mathcal{R}_\beta(\nu-\nu_\circ+m\Delta f)\;e^{j2\pi m\Delta f\tau_l}\end{aligned}\tag{74}$$

Hence, we obtain the following theorem regarding the SNR curve for a radar matched filter approach.

Theorem 7: In the crystalline regime (*i.e.,* when $W_A\gg\Delta f$ and $W_B\gg T$), the SNR curve of the radar matched filter output is given by

$$\begin{aligned}\frac{|r_{\tau,\nu}|^2}{\sigma^2_{\tau,\nu}}\approx\frac{T}{N_0}\sum_{n=-1}^{1}\frac{|\mathcal{R}_\alpha(\tau-\tau_\circ+nT)|^2}{\mathcal{R}_\alpha(0)}\\\sum_{m=-1}^{1}\frac{|\mathcal{R}_\beta(\nu-\nu_\circ+m\Delta f)|^2}{\mathcal{R}_\beta(0)}\end{aligned}\tag{75}$$

$\forall(\tau,\nu)\in[0,T)\times[-\Delta f/2,\Delta f/2)$, for a transmit radar pulse $s(t)=\phi^{g_1}_{\tau_l,\nu_k}(t)$ that is a Type-1 Zak-OTFS pulsone for any $l,k\in\{0,\ldots,M-1\}\times\{0,\ldots,N-1\}$.

Proof: See Appendix E. ■

Remark 9: We note that similar result as Theorem 7 can be obtained for Type-2 Zak-OTFS pulsones, by following the same arguments. Hence, Theorem 7 demonstrates a key property of the Zak-OTFS pulsones, when operating in the crystalline regime. The SNR curve $\frac{|r_{\tau,\nu}|^2}{\sigma^2_{\tau,\nu}}$ is the same for all $l,k\in\{0,\ldots,M-1\}\times\{0,\ldots,N-1\}$, *i.e.,* all input Zak-OTFS pulsones. This result is closely linked to the channel predictability property [8], [9] of Zak-OTFS.

Note that the task of optimal channel tap estimation for the discrete DD domain (*i.e.,* utilizing samples on the grid) was also shown to be linked to radar processing in [13], where discrete DD TC filters were introduced as spreading filters for information symbol spreading in the discrete DD domain leading to *spread pulsones*. A discrete ambiguity function was defined and shown to be the optimal channel tap estimator.

D. ZAK-OTFS RECEIVER MATCHED TO THE TRANSMIT TC FILTER

Now consider a radar sensing setup using a standard Type-1 and Type-2 Zak-OTFS receiver matched to the transmitter, *i.e.,* $g^{\mathrm{Rx}}(\tau,\nu)=(g^{\mathrm{Tx}}(\tau,\nu))^{\dagger}$. Recall that the Zak-OTFS approach for this receive TC filter has a simple implementation using time and frequency windowing as shown in Figure 1. We first note that this Zak-OTFS receiver can be used more generally to sample at an arbitrary point (τ',ν'), that may not be on the transmission DD grid (by computing (25) for (τ',ν') instead of (τ_l,ν_k)).

As in the previous subsection, let the transmitted radar signal $s(t)$ be the Type-1 Zak-OTFS pulsone $\phi^{g_1}_{\tau_l,\nu_k}(t)$. Consider the sample at point $(\tau_l+\tau,\nu_k+\nu)$ given by $\mathcal{Z}_{yg^{\mathrm{Rx}}}(\tau_l+\tau,\nu_k+\nu)$. As before, let $r_{\tau,\nu}$ denote the signal component and $n_{\tau,\nu}$ denote the noise component. The signal component for the Zak-OTFS receiver can be evaluated as

$$\begin{aligned}r_{\tau,\nu}:=e^{-j2\pi\nu_\circ\tau_\circ}\sum_{n\in\mathbb{Z}}\sum_{m\in\mathbb{Z}}\mathcal{Y}_A(\tau-\tau_\circ+nT,-\nu_\circ)e^{-j2\pi\nu_k nT}\\\mathcal{X}_B(-\tau-nT,\nu-\nu_\circ+m\Delta f)\;e^{j2\pi(m\Delta f+\nu)(\tau_l+\tau)}\end{aligned}\tag{76}$$

whereas the noise component can be evaluated as

$$\sigma^2_{\tau,\nu} := \frac{N_0}{T} \sum_{n\in\mathbb{Z}} \sum_{m\in\mathbb{Z}} \mathcal{Y}_A(nT, 0)\ e^{-j2\pi(\nu+\nu_k)nT} \mathcal{X}_B(-nT, m\Delta f) e^{j2\pi m\Delta f(\tau+\tau_l)} \tag{77}$$

In the crystalline regime, using the same arguments as in the previous subsection, the signal component becomes

$$r_{\tau,\nu} \approx e^{-j2\pi\nu_\circ\tau_\circ} \sum_{n=-1}^{1} \mathcal{R}_\alpha(\tau-\tau_\circ+nT)e^{-j2\pi\nu_k nT} \sum_{m=-1}^{1} \mathcal{R}_\beta(\nu-\nu_\circ+m\Delta f)\ e^{j2\pi(m\Delta f+\nu)(\tau_l+\tau)} \tag{78}$$

where as the noise component becomes

$$\sigma^2_{\tau,\nu} \approx \frac{N_0}{T}\mathcal{R}_\alpha(0)\mathcal{R}_\beta(0) \tag{79}$$

By inspection of (78)-(79), note that the Zak-OTFS receiver output SNR $\frac{|r_{\tau,\nu}|^2}{\sigma^2_{\tau,\nu}}$ corresponding to sample at $(\tau_l+\tau, \nu_k+\nu)$ is high when the sampling point is close to the optimal point $(\tau_l+\tau_\circ, \nu_k+\nu_\circ)$, and the SNR is lower further away from this point. This behaviour is very similar to that of the ambiguity function used in the radar approach. We now present a much stronger result about the connection between these two approaches.

The following claim is obtained from (78)-(79) by using similar arguments as in the proof of Theorem 7.

Claim 1: In the crystalline regime (*i.e.,* when $W_A \gg \Delta f$ and $W_B \gg T$), the SNR curve $\frac{|r_{\tau,\nu}|^2}{\sigma^2_{\tau,\nu}}$ for the output of the Zak-OTFS receiver (matched to transmit TC filter) is given by (75) when the transmit radar pulse $s(t)$ is either a Type-1 (or a Type-2) Zak-OTFS pulsone for any $l, k \in \{0, \ldots, M-1\} \times \{0, \ldots, N-1\}$.

We have hence shown that in the crystalline regime, a Type-1 and Type-2 Zak-OTFS based setup (with receive TC filter matched to transmitter) has an identical SNR curve to the radar matched filter, when using a Type-1 (or a Type-2) Zak-OTFS pulsone as the radar pulse.

Remark 10: Claim 1 demonstrates two key properties of the Zak-OTFS pulses (pulsones) in a single target channel.

- In the crystalline regime, the SNR curve $\frac{|r_{\tau,\nu}|^2}{\sigma^2_{\tau,\nu}}$ for a Type-1 and Type-2 Zak-OTFS receiver (matched to transmitter) is the same as the SNR curve for the optimal radar matched filter.
- This SNR curve is the same for all input Zak-OTFS pulsones, *i.e.,* $l, k \in \{0, \ldots, M-1\} \times \{0, \ldots, N-1\}$.

These results imply that a time and frequency windowing based Zak-OTFS receiver can be directly applied for radar sensing with negligible loss in SNR performance, and with the same delay-Doppler resolution.

This also demonstrates the channel predictability property [8], [9] of Type-1 and Type-2 Zak-OTFS, where every input pulse (and the corresponding symbol) undergoes a similar transformation due to the doubly dispersive channel.

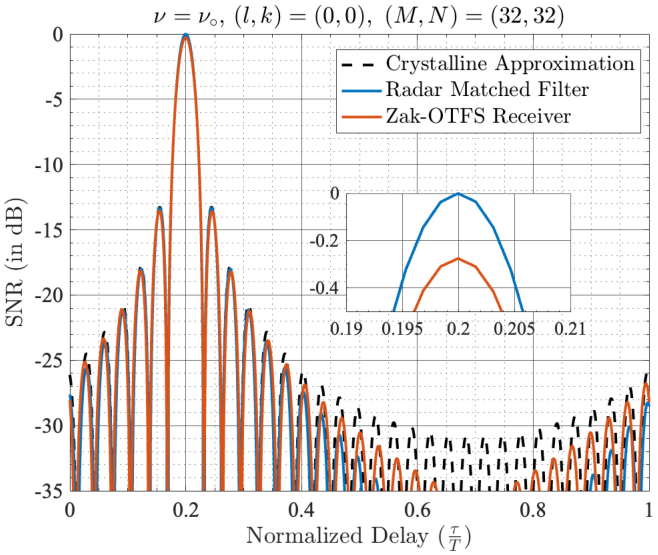

(a) For $(l, k) = (0, 0)$.

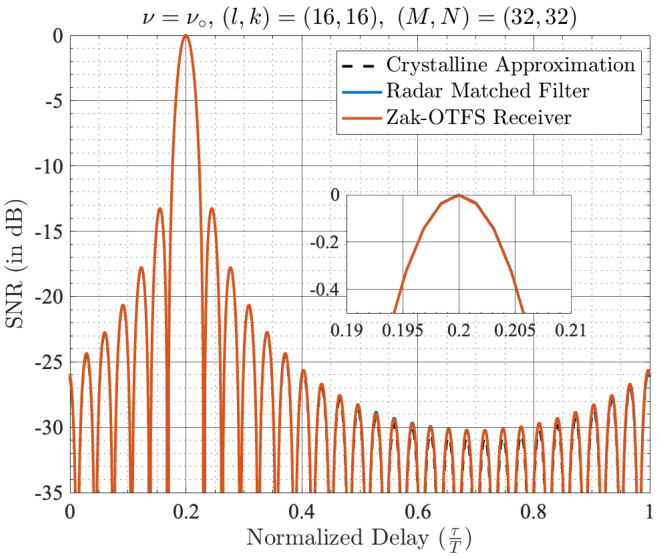

(b) For $(l, k) = (M/2, N/2)$.

FIGURE 5. Delay cut of SNR curve for rectangular windows with $(M, N) = (32, 32)$, for transmit radar signal $\phi^{g_1}_{\tau_l,\nu_k}(t)$. (a) For $(l, k) = (0, 0)$. (b) For $(l, k) = (M/2, N/2)$.

We now compare the SNR curves for the radar approach and the Type-1 and Type-2 Zak-OTFS approach, for rectangular windows with $(M, N) = (32, 32)$. We consider the target location $(\tau_\circ, \nu_\circ) = (0.2T, -0.25\Delta f)$. Figure 5(a) shows the results for a Type-1 pulsone with $(l, k) = (0, 0)$. It can be noted that all three SNR curves are nearly identical and only differ in the sidelobes where the SNR values are very small. The zoomed-in plot shows that the peak SNR of Zak-OTFS receiver is only 0.3 dB less than the optimal value. The results also show that the crystalline approximation is very accurate, even for modest values of M, N.

Figure 5(b) shows the results for Type-1 pulsone with $(l, k) = (16, 16)$. In this case, it can be noted that all three SNR curves are identical. Since the crystalline approximation

does not depend on (l, k), this results illustrates that the actual SNR curves vary slightly around the crystalline approximation for different transmit radar pulses. The variations are negligible as can be noted from Figure 5(a) which presents the worst case.

VIII. IMPLEMENTATION OF THE OPTIMAL ZAK-OTFS RECEIVER FOR SPARSE DOUBLY DISPERSIVE CHANNELS

In this section, we present our implementations of the optimal Zak-OTFS receiver for doubly dispersive channels. The first approach implements the optimal TC filter $(h *_\sigma g^{\mathrm{Tx}})^\dagger(\tau, \nu)$, and we show that this requires radar matched filter processing and computing ambiguity functions with respect to Zak-OTFS transmit pulses. We propose a second implementation that uses the receive TC filter $(g^{\mathrm{Tx}})^\dagger(\tau, \nu)$ that is matched to transmitter and hence only requires time and frequency windowing. We show that the two approaches converge in the crystalline regime. We show that the second implementation is a DD domain rake receiver that coherently combines the multi-path components of the received DD domain signal.

A. CRYSTALLINE REGIME RELATIONSHIP BETWEEN THE OPTIMAL TC FILTER OUTPUT AND TYPE-1 TYPE-2 ZAK-OTFS OUTPUT

Recall from (8) that the Zak-OTFS received signal in the DD domain is $y_{\mathrm{dd}}(\tau, \nu) = h_{\mathrm{dd}} *_\sigma x_{\mathrm{dd}}(\tau, \nu) + n_{\mathrm{dd}}(\tau, \nu)$. Let $r_{\mathrm{dd}}(\tau, \nu) \coloneqq h_{\mathrm{dd}} *_\sigma x_{\mathrm{dd}}(\tau, \nu)$ denote the signal component of $y_{\mathrm{dd}}(\tau, \nu)$.

In this section, we use the following notation to distinguish between the optimal TC filter approach and time-frequency windowing based Zak-OTFS approach.

- We use $(\cdot)^{\mathrm{opt}}_{\mathrm{dd}}(\tau, \nu)$ to denote the DD domain functions/processes corresponding to the optimal receive TC filter $(h *_\sigma g^{\mathrm{Tx}}(\tau, \nu))^\dagger$.
- We use $(\cdot)^{\mathrm{tf}}_{\mathrm{dd}}(\tau, \nu)$ to denote the DD domain functions/processes corresponding to the receive TC filter $(g^{\mathrm{Tx}}(\tau, \nu))^\dagger$ that is matched to the transmit TC filter.

For example, $y^{\mathrm{opt}}_{\mathrm{dd}}(\tau, \nu) = r^{\mathrm{opt}}_{\mathrm{dd}}(\tau, \nu) + n^{\mathrm{opt}}_{\mathrm{dd}}(\tau, \nu)$ denotes the output signal from the optimal TC filter and $y^{\mathrm{tf}}_{\mathrm{dd}}(\tau, \nu) = r^{\mathrm{tf}}_{\mathrm{dd}}(\tau, \nu) + n^{\mathrm{tf}}_{\mathrm{dd}}(\tau, \nu)$ denotes the received signal output after the receiver time-frequency windowing block in Figure 1.

We first present preliminary results required for the main theorem.

Note that for $W_A \gg \Delta f$, $\mathcal{R}_\alpha(\tau) \approx \mathcal{R}_\alpha(\tau) e^{j2\pi\nu\tau}$ for $\nu \in [-\Delta f, \Delta f]$ (by applying Lemma 3 in Appendix F). A similar result can be obtained for $\mathcal{R}_\beta(\nu)$ when $W_B \gg T$ using the same arguments used in Lemma 3. Hence the following assumption about the crystalline regime is justified, and we use it to derive Lemma 2.

Assumption 1: For a transmit TC filter that is of either Type-1 or Type-2, in the crystalline regime, we assume that $\mathcal{R}_\alpha(\tau) \approx e^{j2\pi\nu'\tau}\mathcal{R}_\alpha(\tau)$ and $\mathcal{R}_\beta(\nu) \approx e^{j2\pi\tau'\nu}\mathcal{R}_\beta(\nu)$ for $|\tau'| \le T$ and $|\nu'| \le \Delta f$.

Lemma 2: Let $a(\tau, \nu)$ be a complex valued DD function such that $|a(\tau, \nu)| > 0$ only if $|\tau| \le T, |\nu| \le \Delta f$. Then in the crystalline regime,

$$a *_\sigma \left(g^{Tx}\right)^\dagger *_\sigma g^{Tx}(\tau, \nu) \approx a_{dd}(\tau, \nu) \tag{80}$$

$$\left(g^{Tx}\right)^\dagger *_\sigma g^{Tx} *_\sigma a(\tau, \nu) \approx a_{dd}(\tau, \nu) \tag{81}$$

$$\left(g^{Tx}\right)^\dagger *_\sigma a *_\sigma g^{Tx}(\tau, \nu) \approx a_{dd}(\tau, \nu) \tag{82}$$

under Assumption 1, where

$$a_{dd}(\tau, \nu) \coloneqq e^{j2\pi\nu\tau}\left(a(\tau, \nu)e^{-j2\pi\nu\tau} \star \mathcal{R}_\alpha(\tau)\mathcal{R}_\beta(\nu)\right) \tag{83}$$

and $g^{Tx}(\tau, \nu)$ is either a Type-1 or a Type-2 TC filter.

Proof: See Appendix F. ∎

Remark 11: The twisted convolution operation $*_\sigma$ is not commutative and hence the order of operations cannot be exchanged. In Lemma 2, we have shown that the crystalline regime limit is a special case, where exchange of operations is allowed for (80)-(82). We will now use this property to provide a practical implementation (see Figure 1) of optimal Zak-OTFS receiver using time-frequency windowing based TC filters and Zak domain sampling.

We now present the main theorem about the crystalline regime relationship between the optimal output $y^{\mathrm{opt}}_{\mathrm{dd}}(\tau, \nu)$ and the Type-1, Type-2 output $y^{\mathrm{tf}}_{\mathrm{dd}}(\tau, \nu)$ as the following theorem.

Theorem 8: For a transmit TC filter that is of either Type-1 or Type-2, in the crystalline regime, the two output signals $y^{opt}_{dd}(\tau, \nu)$ and $y^{tf}_{dd}(\tau, \nu)$ are related as follows:

- The noise-free signal components satisfy

$$r^{opt}_{dd}(\tau, \nu) \approx h^\dagger *_\sigma r^{tf}_{dd}(\tau, \nu) \tag{84}$$

- The noise Gaussian processes $n^{opt}_{dd}(\tau, \nu)$ and $n^{tf}_{dd}(\tau, \nu)$ are identically distributed.

Proof: See Appendix F. ∎

We present a comparison of the two approaches before discussing implementation. We consider the Normalized Mean Square Error (NMSE) between the noise-free received symbols of the two approaches as

$$\frac{\sum_{l=0}^{M-1}\sum_{k=0}^{N-1}\left|r^{\mathrm{opt}}_{\mathrm{dd}}[l, k] - h^\dagger *_\sigma r^{\mathrm{tf}}_{\mathrm{dd}}[l, k]\right|^2}{\sum_{l=0}^{M-1}\sum_{k=0}^{N-1}\left|h^\dagger *_\sigma r^{\mathrm{tf}}_{\mathrm{dd}}[l, k]\right|^2} \tag{85}$$

We use numerical simulation for the comparison as follows. We consider a two path channel where the first path has a delay 0 and Doppler shift 0. For the second path, the delay is chosen to be a uniform random variable on interval $[0, T/3)$ and Doppler shift is chosen to be a uniform random variable on interval $[-\Delta f/3, \Delta f/3)$. These values have been chosen to model typical mobile wireless channels, where the channel spreads are small in comparison to the grid dimensions (but can be up to one-third). Note that the crystalline regime conditions hold for these values. For path 1, the path gain is chosen to be a complex Gaussian random

TABLE 3. Simulation parameters.

Parameter	Value
Data Modulation Alphabet	16-QAM
(M, N)	$(32, 32)$
Number of Channel Realizations	10^3

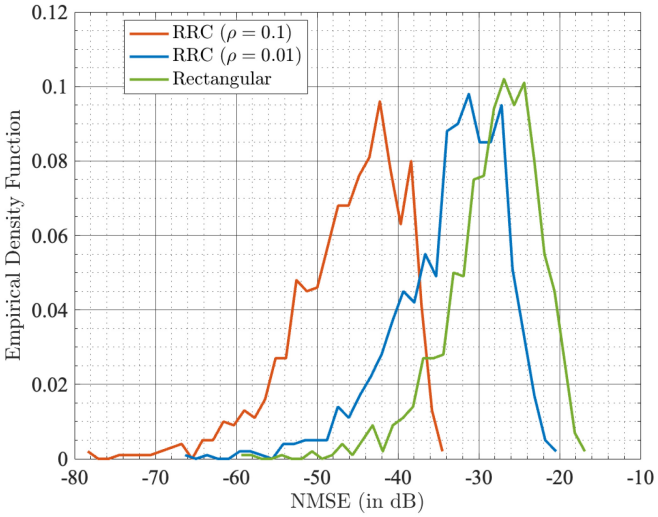

FIGURE 6. NMSE of the received signals between the optimal Zak-OTFS receiver and the crystalline approximation.

variable with zero mean and unit variance, whereas for path 2, the variance is $1/2$. The rest of the simulation parameters are given in Table 3.

Figure 6 presents the NMSE results as an empirical distribution function obtained over channel realizations. It can be seen from the NMSE values are very small for both rectangular and RRC windows. These results indicate that the crystalline approximation approach is nearly identical to the optimal implementation, and that the performance gap is negligible. The NMSE values are much smaller for RRC windows as expected, since they have larger supports compared to rectangular windows.

We now present the optimal receiver implementations corresponding to the two approaches, for sparse doubly dispersive channels. This involves sampling the DD domain signals $y_{\rm dd}^{\rm opt}(\tau, \nu)$ and $y_{\rm dd}^{\rm tf}(\tau, \nu)$ to obtain sufficient statistics.

B. OPTIMAL RECEIVER IMPLEMENTATION FOR A SPARSE DOUBLY DISPERSIVE CHANNEL

Consider the sparse path channel with DD response $h(\tau, \nu) = \sum_{p=0}^{P-1} h_p \delta(\tau - \tau_{l_p})\delta(\nu - \nu_{k_p})$. The Zak-OTFS output for (τ_l, ν_k) corresponding to the optimal TC filter $g^{\rm Rx}(\tau, \nu) := (h *_\sigma g^{\rm Tx}(\tau, \nu))^\dagger$ is equivalent to correlation of the receive signal $y(t)$ with the optimal receive pulse

$$\frac{1}{T}\left(\phi_{\tau_l,\nu_k}^{h*_\sigma g^{\rm Tx}}(t)\right)^* = \frac{1}{T}\sum_{p=0}^{P-1} h_p^* e^{-j2\pi\nu_{k_p}\left(t-\tau_{l_p}\right)}\left(\phi_{\tau_l,\nu_k}^{g^{\rm Tx}}(t-\tau_{l_p})\right)^*.$$

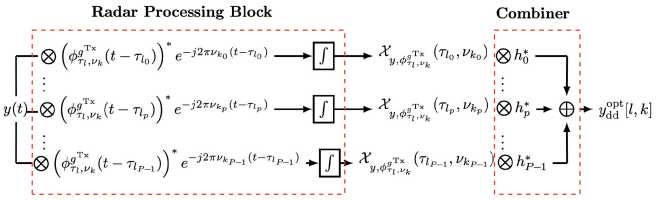

FIGURE 7. Block Diagram for Implementation of the Optimal Receiver.

Hence proceeding similarly as in Section VII-A, the optimal Zak-OTFS receiver output is

$$y_{\rm dd}^{\rm opt}[l,k] = \frac{1}{T}\sum_{p=0}^{P-1} h_p^* \mathcal{X}_{y,\phi_{\tau_l,\nu_k}^{g^{\rm Tx}}}\left(\tau_{l_p}, \nu_{k_p}\right). \tag{86}$$

Figure 7 provides an implementation block diagram of this receiver.

Remark 12: From (86), the optimal Zak-OTFS receiver output sampled at (τ_l, ν_k) is obtained by maximal ratio combining (*i.e.,* according to the conjugates h_p^* of the path gains) the ambiguity function samples $\mathcal{X}_{y,\phi_{\tau_l,\nu_k}^{g^{Tx}}}(\tau_{l_p}, \nu_{k_p})$. As noted in the previous section, these samples can be obtained by radar matched filter processing of $y(t)$ treating $\phi_{\tau_l,\nu_k}^{g^{Tx}}(t)$ as the radar pulse.

Remark 13: Note that in (86) the DD domain sampling is on the integer grid points, as seen from the LHS. However, to evaluate these DD samples in practice, the RHS shows that the ambiguity function needs to be sampled at path locations which will in general be fractional.

C. CRYSTALLINE REGIME IMPLEMENTATION USING TYPE-1 AND TYPE-2 ZAK-OTFS

We can apply Theorem 8 to obtain a time-frequency windowing based receiver as follows:

$$\bar{y}_{\rm dd}^{\rm opt}(\tau, \nu) = h^\dagger *_\sigma y_{\rm dd}^{\rm tf}(\tau, \nu) \tag{87}$$

$$= \sum_{p=0}^{P-1} h_p^* e^{-j2\pi\nu_{k_p}\tau} y_{\rm dd}^{\rm tf}\left(\tau + \tau_{l_p}, \nu + \nu_{k_p}\right) \tag{88}$$

Note that this approach is a DD domain rake receiver as illustrated in Figure 8(a). The multi-path components are being coherently combined to yield the final output.

The sufficient statistics $\bar{y}_{\rm dd}^{\rm opt}[l,k]$ from this time-frequency windowing receiver are obtained by sampling at (τ_l, ν_k) as follows:

$$\bar{y}_{\rm dd}^{\rm opt}[l,k] := \sum_{p=0}^{P-1} h_p^* e^{-j2\pi\nu_{k_p}\tau_l} y_{\rm dd}^{\rm tf}\left(\tau_l + \tau_{l_p}, \nu_k + \nu_{k_p}\right) \tag{89}$$

$$= \sum_{p=0}^{P-1} h_p^* e^{-j2\pi\nu_{k_p}\tau_l} \mathcal{Z}_{y,(g^{\rm Tx})^\dagger}\left(\tau_l + \tau_{l_p}, \nu_l + \nu_{k_p}\right) \tag{90}$$

$\bar{y}_{\rm dd}^{\rm opt}[l,k]$ has the same noise-free signal component as the optimal receiver output $y_{\rm dd}^{\rm opt}[l,k]$ in the crystalline regime, from Theorem 8. Moreover, the noise components $\bar{n}_{\rm dd}^{\rm opt}[l,k]$

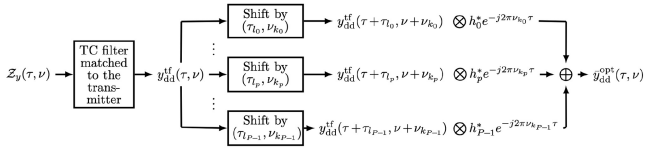

(a) A delay-Doppler Domain Rake Receiver Interpretation of the Type-1 and Type-2 Zak-OTFS Receiver.

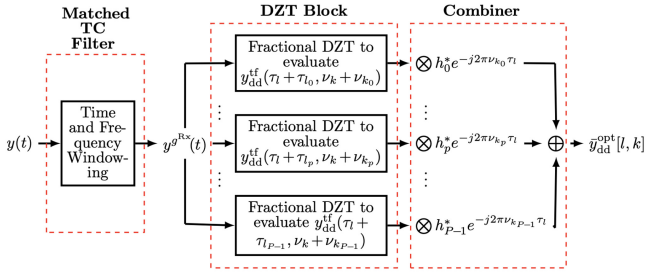

(b) Block Diagram for Implementation of the Type-1 and Type-2 Zak-OTFS Receiver.

FIGURE 8. Optimal Crystalline Regime Implementation using Type-1 and Type-2 Zak-OTFS Receiver.

and $n_{\rm dd}^{\rm opt}[l,k]$ have an identical distribution from Theorem 8. This shows that they also form the sufficient statistics for ML detection. An implementation block diagram for this receiver is shown in Figure 8(b).

Remark 14: From (90), in the crystalline regime, the optimal Zak-OTFS receiver output for (l,k) can be obtained by maximal ratio combining (*i.e.,* according to (90)) the Zak-OTFS output samples $\mathcal{Z}_{y(g^{Tx})^\dagger}(\tau_l+\tau_{l_p}, \nu_l+\nu_{k_p})$ using the receive TC filter $(g^{Tx})^\dagger(\tau,\nu)$, when the transmit TC filter is of either Type-1 or Type-2.

This proposed Zak-OTFS implementation is a delay-Doppler rake receiver, where a symbol $\bar{y}^{opt}[l,k]$ is obtained by coherently combining the samples $\mathcal{Z}_{y(g^{Tx})^\dagger}(\tau_l+\tau_{l_p}, \nu_l+\nu_{k_p})$ corresponding to each path $p=0,\ldots,P-1$ according to a maximum ratio combining criterion.

D. OPTIMAL RECEIVER IMPLEMENTATION CHALLENGES

In the crystalline regime, we have shown that it is possible to obtain the sufficient statistics for Zak-OTFS using time and frequency windowing based TC filter implementations. Under this proposed Zak-OTFS implementation, a symbol $\bar{y}^{\rm opt}[l,k]$ is obtained by coherently combining the samples $\mathcal{Z}_{y(g^{Tx})^\dagger}(\tau_l+\tau_{l_p}, \nu_l+\nu_{k_p})$ corresponding to each path $p=0,\ldots,P-1$ according to a maximum ratio combining criterion. Hence, each of the MN output symbols $\bar{y}^{\rm opt}[l,k]$ requires combining P DD domain samples.

In the case where the path DD parameters are integer valued and line up with the DD transmission grid, the sufficient statistics can be computed from the samples taken on the integer points as in (25), and fractional samples are not required. However in general, when the path parameters are non-integer valued, samples taken between the grid points are required to compute the sufficient statistics, under this time-frequency based TC filter implementation.

Hence, finer sampling (*i.e.,* oversampling) between the grid points is required to get accurate measurements of output sample values corresponding to path locations $(\tau_l+\tau_{l_p}, \nu_k+\nu_{k_p})$, which increases the receiver complexity. This is also the case for the optimal radar matched filtering implementation, see Remark 13. This also means that obtaining more measurements by sampling between the grid points can potentially yield more capacity. Early investigations into such fractional sampling based receiver architectures were considered for MC-OTFS [16], [17].

The other challenges are channel estimation to obtain channel information regarding the path parameters to get $h(\tau,\nu)$, and a computationally efficient algorithm for performing ML detection. These challenges have been considered before, for the case of integer sampling on transmission grid. For channel estimation, sparse Bayesian learning based models were proposed to estimate the Doppler shifts from the received OTFS pilot symbols [18], [19], [20]. For OTFS ML detection, message passing based detectors have been proposed [4], [21], [22], [23], [24], [25].

IX. CONCLUSION

The conclusions of the paper are as follows:

- We have shown that a Zak-OTFS receiver is equivalent to a correlation demodulator (in Theorem 1) in Section III-A. We have also formulated the concept of a DD domain matched TC filter and derived its structure (in Theorem 2) in Section III-B.
- We have shown that a TC filtered white noise process is a Gaussian process in the DD domain and also derived its DD domain covariance function (in Theorem 3) in Section IV-A. We have also derived a DD domain input-output relationship for TC filtered noise processes (in Remark 6) in Section IV-C.
- For doubly dispersive channels, we have defined a optimal receive TC filter that is matched to the twisted convolution of the channel with the transmit TC filter (in Section V). We have shown that this optimal receive TC filter, sampled at the DD grid points is the optimal Zak-OTFS receiver that recovers sufficient statistics for maximum likelihood detection of the data symbols (in Theorem 5).
- We have derived the effective channel response of Type-1 and Type-2 Zak-OTFS implementations, where the receiver is matched to the transmit TC filter in Section VI. We have also derived the limiting effective channel response for the crystalline regime limit.
- We have derived the crystalline regime SNR curve for the radar matched filter approach that uses a Type-1 (or a Type-2) Zak-OTFS transmit radar pulse (in Theorem 7) in Section VII-C. We have shown that a Zak-OTFS receiver approach that is matched to the transmitter, has an identical crystalline regime SNR curve for radar sensing (in Claim 1) in Section VII-D.
- We have derived the crystalline regime relationship between the outputs of the optimal Zak-OTFS receiver

(that is matched to both the channel and the transmitter) and the Zak-OTFS receiver that is only matched to the transmitter, in Theorem 8 in Section VIII-A.

- We have presented two implementations of the optimal Zak-OTFS receiver in Section VIII. The first implementation of the optimal Zak-OTFS receiver requires radar matched filter processing and involves computing ambiguity functions with respect to Zak-OTFS transmit pulsones. The second implementation is a DD domain rake receiver, that requires only time and frequency windowing and discrete Zak transform computations.

APPENDIX A
PROOFS OF THEOREM 1 AND THEOREM 2

Proof of Theorem 1: From the definition of Zak transform in (26), we obtain

$$\mathcal{Z}_{y^g}(\tau,\nu) \coloneqq \int y^g(t)\psi_{\tau,\nu}(t)dt$$

By definition of $y^g(t)$ in (11), we obtain

$$\mathcal{Z}_{y^g}(\tau,\nu) = \int\iint g(\tau',\nu')y(t-\tau')e^{j2\pi\nu'(t-\tau')}d\tau' d\nu'\psi_{\tau,\nu}(t)dt$$

By defining $t' \coloneqq t-\tau'$ and substituting $t = t'+\tau'$, we get

$$\mathcal{Z}_{y^g}(\tau,\nu) = \int y(t')\iint g(\tau',\nu')e^{j2\pi\nu' t'}\psi_{\tau,\nu}(t'+\tau')d\tau' d\nu' dt'$$

Now by substituting $g(\tau',\nu') = \tilde{g}(-\tau',\nu')e^{j2\pi\nu'\tau'}$ from (29), and by defining $\tau'' \coloneqq -\tau'$, we obtain

$$\begin{aligned}\mathcal{Z}_{y^g}(\tau,\nu) &= \int y(t')\iint \tilde{g}(\tau'',\nu')\psi_{\tau,\nu}(t'-\tau'')e^{j2\pi\nu'(t-\tau'')}d\tau'' d\nu' dt' \\ &= \int y(t')\ \tilde{g}*_\sigma \psi_{\tau,\nu}(t')dt'\end{aligned}$$

which completes the proof. ∎

Proof of Theorem 2: Note that by choosing $g^{\mathrm{Rx}}(\tau,\nu) = (g^{\mathrm{Tx}}(\tau,\nu))^\dagger$, $\tilde{g}^{\mathrm{Rx}}(\tau,\nu) = (g^{\mathrm{Tx}}(\tau,-\nu))^*$. Also note $\psi_{\tau_l,\nu_k}(t) = \frac{1}{T}(\phi_{\tau_l,\nu_k}(t))^*$ from (27). Hence by Definition 3, we obtain that $\psi^{\tilde{g}^{\mathrm{Rx}}}_{\tau_l,\nu_k}(t) = \frac{1}{T}(g^{\mathrm{Tx}}(\tau,-\nu))^* *_\sigma \phi^*_{\tau_l,\nu_k}(t)$ which can be evaluated as

$$\iint \left(g^{\mathrm{Tx}}(\tau',-\nu')\right)^* \frac{\phi^*_{\tau_l,\nu_k}(t-\tau')}{T}e^{j2\pi\nu'(t-\tau')}d\tau' d\nu'$$

By replacing ν' with $-\nu''$, we obtain

$$\left(\iint g^{\mathrm{Tx}}(\tau',\nu'')\frac{\phi_{\tau_l,\nu_k}(t-\tau')}{T}e^{j2\pi\nu''(t-\tau')}d\tau' d\nu''\right)^*$$

Hence from (11), $\psi^{\tilde{g}^{\mathrm{Rx}}}_{\tau_l,\nu_k}(t) = \frac{1}{T}(g^{\mathrm{Tx}} *_\sigma \phi_{\tau_l,\nu_k}(t))^*$. This proves the theorem from (35). ∎

APPENDIX B
PROOF OF THEOREM 3

Proof of Theorem 3.1: Consider the band-limited Gaussian sinc process

$$n_W(t) \coloneqq \sum_{i\in\mathbb{Z}} X_i\kappa_i^{(W)}(t) \tag{91}$$

where X_i's are *i.i.d* Gaussian random variables with zero mean and variance N_0, and the sinc function $\kappa_i^{(W)}(t) \coloneqq \sqrt{2W}\mathrm{sinc}(2Wt-i)$ is bandlimited on $[-W,W]$ in the frequency domain. The white noise process $n(t)$ is the limit of the Gaussian sinc process $\lim_{W\to\infty} n_W(t)$, since $\mathbb{E}[n_W(t_1)n_W(t_2)] = 2N_0W\mathrm{sinc}(2W(t_1-t_2))$ which tends to $N_0\delta(t_1-t_2)$ as $W\to\infty$, for all $t_1,t_2\in\mathbb{R}$.

We will show that for any $W>0$, the TC filtered Gaussian sinc process $\mathcal{Z}_{n^g_W}(\tau,\nu)$ is a zero mean Gaussian process, which completes the proof. From Theorem 1, note that

$$\mathcal{Z}_{n^g_W}(\tau,\nu) = \int n_W(t)\psi^{\tilde{g}}_{\tau,\nu}(t)dt = \sum_{i\in\mathbb{Z}} X_i a_i(\tau,\nu) \tag{92}$$

where $a_i(\tau,\nu) \coloneqq \int \kappa_i^{(W)}(t)\psi^{\tilde{g}}_{\tau,\nu}(t)dt$.

Provided $\sum_{i\in\mathbb{Z}}|a_i(\tau,\nu)|^2 < \infty$ for all $(\tau,\nu)\in\mathbb{R}^2$, any finite vector $[\mathcal{Z}_{n^g_W}(\tau_k,\nu_k)]_{k=0}^K$ is jointly Gaussian distributed (and equivalently $\mathcal{Z}_{n^g_W}(\tau,\nu)$ is a Gaussian process), using the arguments of [14, Th. 3.6.10]. Note that since $\mathbb{E}[|\mathcal{Z}_{n^g_W}(\tau,\nu)|^2] = N_0\sum_{i\in\mathbb{Z}}|a_i(\tau,\nu)|^2$, it is sufficient to show that variance of $\mathcal{Z}_{n^g_W}(\tau,\nu)$ is finite for all (τ,ν), which we do so as follows. From (92) and from the fact that $\mathbb{E}[n_W(t_1)n^*_W(t_2)] = 2N_0W\mathrm{sinc}(2W(t_1-t_2))$, we get

$$\begin{aligned}\mathbb{E}\left[\left|\mathcal{Z}_{n^g_W}(\tau,\nu)\right|^2\right] &= \mathbb{E}\left[\left|\int n_W(t)\psi^{\tilde{g}}(t)dt\right|^2\right] \\ &= 2N_0W\iint \mathrm{sinc}(2W(t-t'))\left(\psi^{\tilde{g}}_{\tau,\nu}(t)\right)^*\psi^{\tilde{g}}_{\tau,\nu}(t')dtdt' \\ &= 2N_0W\int \mathrm{sinc}(2Wt'')\int \psi^{\tilde{g}}_{\tau,\nu}(t')\left(\psi^{\tilde{g}}_{\tau,\nu}(t'+t'')\right)^* dt'dt'' \\ &= 2N_0W\int \mathrm{sinc}(2Wt'')\mathcal{R}_{\psi^{\tilde{g}}_{\tau,\nu}}(-t'')dt''\end{aligned}$$

where $\mathcal{R}_s(\tau)$ represents the auto-correlation function of $s(t)$.

We apply Plancherel's theorem to get

$$\begin{aligned}\mathbb{E}\left[\left|\mathcal{Z}_{n^g_W}(\tau,\nu)\right|^2\right] &= N_0\int_{-W}^{W}\left|\Psi^{\tilde{g}}_{\tau,\nu}(-f)\right|^2 df \\ &\le N_0\int\left|\Psi^{\tilde{g}}_{\tau,\nu}(f)\right|^2 df\end{aligned}$$

where $\Psi^{\tilde{g}}_{\tau,\nu}(f)$ is the Fourier transform of $\psi^{\tilde{g}}_{\tau,\nu}(t)$. Now by Parseval's theorem, $\mathbb{E}[|\mathcal{Z}_{n^g_W}(\tau,\nu)|^2] \le N_0\int\left|\psi^{\tilde{g}}_{\tau,\nu}(t)\right|^2 dt$, which completes the proof by square integrability of $\psi^{\tilde{g}}_{\tau,\nu}(t)$. ∎

Proof of Theorem 3.2: Note that $\mathcal{Z}_{n^g}(\tau,\nu) = \int n(t)\psi^{\tilde{g}}_{\tau,\nu}(t)dt$ from Theorem 1. Hence, the covariance

function $C_{\mathcal{Z}_{ng}}(\tau,\nu|\tau',\nu')$

$$= \iint \mathbb{E}\big[n(t)n^*(t')\big]\psi^{\tilde{g}}_{\tau,\nu}(t)\Big(\psi^{\tilde{g}}_{\tau',\nu'}(t')\Big)^* dtdt'$$

Now since $\mathbb{E}[n(t)n^*(t')] = N_0\delta(t-t')$ and since $(\psi^{\tilde{g}}_{\tau',\nu'}(t'))^* = \frac{1}{T}\phi^{g^\dagger}_{\tau,\nu}(t')$ from (37) of Theorem 2, we obtain

$$C_{\mathcal{Z}_{ng}}(\tau,\nu|\tau',\nu') = \frac{N_0}{T}\int \psi^{\tilde{g}}_{\tau,\nu}(t)\phi^{g^\dagger}_{\tau',\nu'}(t)dt.$$

Note that $\int s(t)\psi^{\tilde{g}}_{\tau,\nu}(t)dt = \mathcal{Z}_{sg}(\tau,\nu) = g *_\sigma \mathcal{Z}_s(\tau,\nu)$ from Theorem 1. Hence, $\int \psi^{\tilde{g}}_{\tau,\nu}(t)\phi^{g^\dagger}_{\tau',\nu'}(t)dt = g *_\sigma \mathcal{Z}_{\phi^{g^\dagger}_{\tau',\nu'}}(\tau,\nu)$ $= g *_\sigma g^\dagger *_\sigma \mathcal{Z}_{\phi_{\tau',\nu'}}(\tau,\nu)$ which completes the proof. ■

APPENDIX C
PROOF OF THEOREM 5

Proof of Theorem 5: From Theorem 1, the Zak-OTFS receiver outputs for a receive TC filter $g^{\mathrm{Rx}}(\tau,\nu)$ are

$$\mathcal{Z}_{yg^{\mathrm{Rx}}}(\tau_l,\nu_k) = \int y(t)\psi^{\tilde{g}^{\mathrm{Rx}}}_{\tau_l,\nu_k}(t)dt$$

Since $g^{\mathrm{Rx}}(\tau,\nu) = (h *_\sigma g^{\mathrm{Tx}}(\tau,\nu))^\dagger$, using (37) of Theorem 2, we obtain that $\psi^{\tilde{g}^{\mathrm{Rx}}}_{\tau_l,\nu_k}(t) = \frac{1}{T}(\phi^{h*_\sigma g^{\mathrm{Tx}}}_{\tau_l,\nu_k}(t))^*$. Hence,

$$\mathcal{Z}_{yg^{\mathrm{Rx}}}(\tau_l,\nu_k) = \frac{1}{T}\int y(t)\Big(\phi^{h*_\sigma g^{\mathrm{Tx}}}_{\tau_l,\nu_k}(t)\Big)^* dt = \frac{1}{T}y^{\mathrm{opt}}[l,k].$$

provide sufficient statistics for ML detection. ■

APPENDIX D
PROOFS OF THEOREM 6 AND LEMMA 1

Proof of Theorem 6: Note that for Type-1 implementation, $h_{\mathrm{dd}}(\tau,\nu) := g_2^{\mathrm{Rx}} *_\sigma h *_\sigma g_1^{\mathrm{Tx}}(\tau,\nu)$, where the TC filters $g_2^{\mathrm{Rx}}(\tau,\nu) = \alpha^{\mathrm{Rx}}(\tau)\beta^{\mathrm{Rx}}(\nu)e^{j2\pi\nu\tau}$ and $g_1^{\mathrm{Tx}}(\tau,\nu) = \alpha^{\mathrm{Tx}}(\tau)\beta^{\mathrm{Tx}}(\nu)$.

We evaluate $h *_\sigma g_1^{\mathrm{Tx}}(\tau,\nu)$ as

$$h *_\sigma g_1^{\mathrm{Tx}}(\tau,\nu) = \iint h(\tau',\nu')\,\alpha^{\mathrm{Tx}}(\tau-\tau')\beta^{\mathrm{Tx}}(\nu-\nu')e^{j2\pi\nu'(\tau-\tau')}d\tau'd\nu' \tag{93}$$

Using this, we evaluate $h_{\mathrm{dd}}(\tau,\nu) = g_2^{\mathrm{Rx}} *_\sigma (h *_\sigma g_1^{\mathrm{Tx}})(\tau,\nu)$ as

$$h_{\mathrm{dd}}(\tau,\nu) = \iint h(\tau',\nu')e^{j2\pi\nu'(\tau-\tau')} \underbrace{\left(\int \alpha^{\mathrm{Rx}}(\tau_\circ)\alpha^{\mathrm{Tx}}(\tau-\tau_\circ-\tau')e^{-j2\pi\tau_\circ\nu'}d\tau_\circ\right)}_{\text{Integral-1}} \underbrace{\left(\int \beta^{\mathrm{Rx}}(\nu_\circ)\beta^{\mathrm{Tx}}(\nu-\nu_\circ-\nu')e^{j2\pi\nu_\circ\tau}d\nu_\circ\right)}_{\text{Integral-2}} d\tau'd\nu' \tag{94}$$

By denoting $\underline{\alpha}^{\mathrm{Rx}}(\tau) := (\alpha^{\mathrm{Rx}}(-\tau))^*$ and defining $t := \tau-\tau_\circ-\tau'$, we evaluate Integral-1 as

$$-\left(\int \alpha^{\mathrm{Tx}}(t)\big(\underline{\alpha}^{\mathrm{Rx}}(t-(\tau-\tau'))\big)^* e^{j2\pi\nu'(t-(\tau-\tau'))}dt\right) = -\mathcal{X}_{\alpha^{\mathrm{Tx}},\underline{\alpha}^{\mathrm{Rx}}}(\tau-\tau',-\nu') = -\mathcal{Y}_{A^{\mathrm{Tx}},(A^{\mathrm{Rx}})^*}(\tau-\tau',-\nu')$$

where the final step is due to the fact that α^{Tx} and A^{Tx} are a Fourier pair, and so are $\underline{\alpha}^{\mathrm{Rx}}$ and $(A^{\mathrm{Rx}})^*$.

By denoting $\underline{\beta}^{\mathrm{Rx}}(\nu) := (\beta^{\mathrm{Rx}}(-\nu))^*$ and by defining $f := \nu-\nu_\circ-\nu'$, we evaluate Integral-2 as

$$\begin{aligned}&-\left(\int \beta^{\mathrm{Tx}}(f)\Big(\underline{\beta}^{\mathrm{Rx}}\big(f-(\nu-\nu')\big)\Big)^* e^{-j2\pi\tau(f-(\nu-\nu'))}df\right)\\ &= -\mathcal{Y}_{\beta^{\mathrm{Tx}},\underline{\beta}^{\mathrm{Rx}}}(-\tau,\nu-\nu')e^{j2\pi\tau(\nu-\nu')}\\ &= -\mathcal{X}_{B^{\mathrm{Tx}},(B^{\mathrm{Rx}})^*}(-\tau,\nu-\nu')e^{j2\pi\tau(\nu-\nu')}\end{aligned}$$

where the final step is due to the fact that β^{Tx} and B^{Tx} are a Fourier pair, and so are $\underline{\beta}^{\mathrm{Rx}}$ and $(B^{\mathrm{Rx}})^*$.

The proof for Type-1 $\overline{\text{Z}}$ak-OTFS is complete now by substituting Integral-1 and Integral-2 into (94). The result for Type-2 Zak-OTFS can be obtained by evaluating the twisted convolutions and then using same arguments. ■

Proof of Lemma 1: We first show that $\mathcal{Y}_{A_1}(\tau,\nu)$ is 0.5-Hölder continuous along ν. For $\varepsilon > 0$, note that by Cauchy-Schwarz inequality,

$$\begin{aligned}&\big|\mathcal{Y}_{A_1}(\tau,\nu)-\mathcal{Y}_{A_1}(\tau,\nu+\varepsilon)\big|^2\\ &= \left|\int A_1(f)\big(A_1^*(f-\nu)-A_1^*(f-\nu-\epsilon)\big)e^{j2\pi f\tau}df\right|^2\\ &\le \int |A_1(f)|^2df\int\big|\big(A_1^*(f-\nu)-A_1^*(f-\nu-\epsilon)\big)\big|^2df\\ &= \left(\int |A_1(f)|^2df\right)\big(2\mathrm{Re}\big(\mathcal{R}_{A_1}(0)-\mathcal{R}_{A_1}(\varepsilon)\big)\big)\end{aligned}$$

where $\mathrm{Re}(\cdot)$ represents the real part of a complex number.

Since $A_1(f)$ is square integrable and by Lipschitz continuity of $\mathcal{R}_{A_1}(\cdot)$, we obtain that $\mathcal{Y}_{A_1,A_1}(\tau,\nu)$ is 0.5-Hölder continuous, *i.e.*, $\exists K_{A_1} > 0$ such that

$$\big|\mathcal{Y}_{A_1}(\tau,\nu)-\mathcal{Y}_{A_1}(\tau,\nu+\varepsilon)\big| \le K_{A_1}\sqrt{|\varepsilon|},\ \ \forall\varepsilon\in\mathbb{R}$$

Hence we have

$$\left|\mathcal{Y}_{A_1}\Big(\tau W,\frac{\nu}{W}\Big)-\mathcal{Y}_{A_1}(\tau W,0)\right| \le K_{A_1}\sqrt{|\nu|/W},$$

$\forall W > 1$. Now since $\mathcal{Y}_{A_1}(\tau W,\frac{\nu'}{W}) = \mathcal{Y}_{A_W}(\tau,\nu')$, we obtain

$$\big|\mathcal{Y}_{A_W}(\tau,\nu)-\mathcal{Y}_{A_W}(\tau,0)\big| \le K_{A_1}\sqrt{|\nu|/W} \tag{95}$$

Note that from (44) that $\mathcal{Y}_{A_W}(0,\nu)$ is the inverse Fourier transform of $|A_W(f)|^2$ and equals $\mathcal{R}_{\alpha_W}(\tau)$. This completes the proof. ■

APPENDIX E
PROOF OF THEOREM 7

Proof of Theorem 7: For Type-1 pulsone, note from (74) that $\left|\mathcal{X}_{s,s}(\tau,\nu)\right|^2$ equals

$$T^2\left(\sum_{n=-1}^{1}\sum_{n'=-1}^{1}\mathcal{R}_\alpha(\tau+nT)\mathcal{R}_\alpha^*\left(\tau+n'T\right)e^{-j2\pi\nu_k(n-n')T}\right)\left(\sum_{m=-1}^{1}\sum_{m'=-1}^{1}\mathcal{R}_\beta(\nu+m\Delta f)\ \mathcal{R}_\beta^*\left(\nu+m'\Delta f\right)e^{j2\pi\tau_l(m-m')\Delta f}\right)$$

Since $W_A \gg \Delta f$ and $W_B \gg T$, note that $\mathcal{R}_\alpha(\tau+nT)\mathcal{R}_\alpha^*(\tau+n'T) \approx 0$ for $n \neq n'$ and $\mathcal{R}_\beta(\nu+m\Delta f)\ \mathcal{R}_\beta^*(\nu+m'\Delta f) \approx 0$ for $m \neq m'$. Hence,

$$\frac{\left|\mathcal{X}_{s,s}(\tau,\nu)\right|^2}{T^2} \approx \sum_{n=-1}^{1}|\mathcal{R}_\alpha(\tau+nT)|^2\sum_{m=-1}^{1}\left|\mathcal{R}_\beta(\nu+m\Delta f)\right|^2 \tag{96}$$

Since $\sigma_{\tau,\nu}^2 = N_0\mathcal{X}_{s,s}(0,0)$, note from (74) that

$$\frac{\sigma_{\tau,\nu}^2}{N_0T} \approx \sum_{n=-1}^{1}\mathcal{R}_\alpha(nT)e^{-j2\pi\nu_k nT}\sum_{m=-1}^{1}\mathcal{R}_\beta(m\Delta f)\ e^{-j2\pi\tau_l m\Delta f}$$

Since $W_A \gg \Delta f$ and $W_B \gg T$ $R_\alpha(\tau) \approx 0, \forall\tau{:}|\tau| > T$ and $R_\beta(\nu) \approx 0, \forall\nu{:}|\nu| > \Delta f$. Hence, $\sigma_{\tau,\nu}^2 \approx N_0T\mathcal{R}_\alpha(0)\mathcal{R}_\beta(0)$.

Hence from (72) and (96), it follows that the Theorem holds when the radar transmit pulse is a Type-1 pulsone.

The proof follows from similar arguments for a Type-2 pulsone. ∎

APPENDIX F
LEMMA 3 AND PROOFS OF LEMMA 2 AND THEOREM 8

Lemma 3: Consider a family of window functions $\{A_W(f)\}_{W\geq 1}$, where $A_W(f) := \sqrt{\frac{1}{W}}A_1(\frac{f}{W})$, formed from a prototype unit window $A_1(f)$ that has unit support. $A_W(f)$ is the scaled window that has support W with the same energy and shape as $A_1(f)$. Then the error $\epsilon_W(\tau,\nu) := \left|e^{j2\pi\nu\tau}\mathcal{R}_{\alpha_W}(\tau) - \mathcal{R}_{\alpha_W}(\tau)\right|$ satisfies

$$\max_{\tau\in\mathbb{R}}\epsilon_W(\tau,\nu) \leq K_{A_1}\frac{\Delta f}{W}. \tag{97}$$

for some constant $K_{A_1} > 0$.

Proof: Note that the error can be expressed as $\epsilon_W(\tau,\nu) = \left|\mathcal{R}_{\alpha_W}(\tau)\sin(\pi\nu\tau)\right|$. Since $|\sin(x)| \leq |x|$, we obtain

$$\max_{\nu\in[-\Delta f,\Delta f]}\epsilon_W(\tau,\nu) < \left|\mathcal{R}_{\alpha_W}(\tau)\pi\Delta f\tau\right|$$

Note that since $\mathcal{R}_{\alpha_W}(\tau)$ is the inverse Fourier transform of $\frac{1}{W}\left|A(\frac{f}{W})\right|^2$, it follows that $\mathcal{R}_{\alpha_W}(\tau) = \mathcal{R}_{\alpha_1}(W\tau)$. Hence,

$$\max_{\tau\in\mathbb{R}}\epsilon_W(\tau,\nu) \leq \frac{\Delta f}{W}\max_{\tau'\in\mathbb{R}}\left|\pi\tau'\mathcal{R}_{\alpha_1}(\tau')\right|$$

Note that $\lim_{\tau\to\infty}\tau\mathcal{R}_{\alpha_1}(\tau)$ must be finite, since otherwise $\mathcal{R}_{\alpha_1}(\tau)$ would not be square integrable. Hence, $\max_{\tau'}\left|\pi\tau'\mathcal{R}_{\alpha_1}(\tau')\right|$ must be finite and can be taken to be the constant K_{A_1}. ∎

Proof of Lemma 2: It can be shown that $(g^{\mathrm{Tx}})^\dagger *_\sigma g^{\mathrm{Tx}}(\tau,\nu) = e^{j2\pi\nu\tau}\mathcal{R}_\alpha(\tau)\mathcal{X}_B(-\tau,\nu)$ for a Type-1 TC filter and $(g^{\mathrm{Tx}})^\dagger *_\sigma g^{\mathrm{Tx}}(\tau,\nu) = e^{j2\pi\nu\tau}\mathcal{R}_\beta(\nu)\mathcal{Y}_A(\tau,-\nu)$ for a Type-2 TC filter. Hence in the crystalline regime, we can take

$$\left(g^{\mathrm{Tx}}\right)^\dagger *_\sigma g^{\mathrm{Tx}}(\tau,\nu) \approx e^{j2\pi\nu\tau}\mathcal{R}_\alpha(\tau)\mathcal{R}_\beta(\nu) \tag{98}$$

Hence, $a *_\sigma (g^{\mathrm{Tx}})^\dagger *_\sigma g^{\mathrm{Tx}}(\tau,\nu) = e^{j2\pi\nu\tau}\iint h(\tau',\nu')e^{-j2\pi\nu\tau'}\mathcal{R}_\alpha(\tau-\tau')\mathcal{R}_\beta(\nu-\nu')d\tau'd\nu'$. (80) now follows by replacing $\mathcal{R}_\beta(\nu-\nu')$ with $e^{j2\pi\tau'(\nu-\nu')}\mathcal{R}_\beta(\nu-\nu')$, using Assumption 1.

Similarly, $(g^{\mathrm{Tx}})^\dagger *_\sigma g^{\mathrm{Tx}} *_\sigma a(\tau,\nu) \approx e^{j2\pi\nu\tau}\iint a(\tau',\nu')e^{-j2\pi\nu'\tau'}e^{-j2\pi\nu'(\tau-\tau')}\mathcal{R}_\alpha(\tau-\tau')\mathcal{R}_\beta(\nu-\nu')d\tau'd\nu'$. (81) follows by replacing $e^{-j2\pi\nu'(\tau-\tau')}\mathcal{R}_\alpha(\tau-\tau')$ with $\mathcal{R}_\alpha(\tau-\tau')$, using Assumption 1.

For (82), note that it is equivalent to Corollary 3. ∎

Proof of Theorem 8: Since for the optimal TC filter case, the receive TC filter is $(h *_\sigma g^{\mathrm{Tx}})^\dagger(\tau,\nu)$ and the transmit TC filter is $g^{\mathrm{Tx}}(\tau,\nu)$, from (9), we obtain $h_{\mathrm{dd}}^{\mathrm{opt}}(\tau,\nu) = (h *_\sigma g^{\mathrm{Tx}})^\dagger *_\sigma h *_\sigma g^{\mathrm{Tx}}(\tau,\nu) = (g^{\mathrm{Tx}})^\dagger *_\sigma h^\dagger *_\sigma h *_\sigma g^{\mathrm{Tx}}(\tau,\nu)$. Similarly for the time-frequency windowing case, $h_{\mathrm{dd}}^{\mathrm{tf}}(\tau,\nu) = (g^{\mathrm{Tx}})^\dagger *_\sigma h *_\sigma g^{\mathrm{Tx}}(\tau,\nu)$. Hence by using Lemma 2,

$$\begin{aligned} h_{\mathrm{dd}}^{\mathrm{opt}}(\tau,\nu) &\approx h^\dagger *_\sigma h *_\sigma \left(g^{\mathrm{Tx}}\right)^\dagger *_\sigma g^{\mathrm{Tx}}(\tau,\nu) \\ &\approx h^\dagger *_\sigma \left(g^{\mathrm{Tx}}\right)^\dagger *_\sigma h *_\sigma g^{\mathrm{Tx}}(\tau,\nu) \\ &= h^\dagger *_\sigma h_{\mathrm{dd}}^{\mathrm{tf}}(\tau,\nu) \end{aligned} \tag{99}$$

Now since $r_{\mathrm{dd}}^{\mathrm{opt}}(\tau,\nu) := h_{\mathrm{dd}}^{\mathrm{opt}} *_\sigma x_{\mathrm{dd}}(\tau,\nu)$ and $r_{\mathrm{dd}}^{\mathrm{tf}}(\tau,\nu) := h_{\mathrm{dd}}^{\mathrm{tf}} *_\sigma x_{\mathrm{dd}}(\tau,\nu)$, it is clear that

$$r_{\mathrm{dd}}^{\mathrm{opt}}(\tau,\nu) \approx h^\dagger *_\sigma r_{\mathrm{dd}}^{\mathrm{tf}}(\tau,\nu) \tag{100}$$

We will now show that the covariance functions of the two noise Gaussian processes $n_{\mathrm{dd}}^{\mathrm{opt}}(\tau,\nu)$ and $h^\dagger *_\sigma n_{\mathrm{dd}}^{\mathrm{tf}}(\tau,\nu)$ are the same. This completes the proof since for a Gaussian process, the mean and the covariance function fully characterize the distributions (see [14, Th. 3.6.3]).

Consider the noise covariance function of zero mean Gaussian process $n_{\mathrm{dd}}^{\mathrm{opt}}(\tau,\nu) := (h *_\sigma g^{\mathrm{Tx}})^\dagger *_\sigma \mathcal{Z}_n(\tau,\nu)$. From (53) of Remark 6, we have

$$\begin{aligned} &C_{n_{\mathrm{dd}}^{\mathrm{opt}}}\left(\tau,\nu|\tau',\nu'\right) \\ &\quad= \left(h *_\sigma g^{\mathrm{Tx}}\right)^\dagger *_\sigma h *_\sigma g^{\mathrm{Tx}} *_\sigma C_{\mathcal{Z}_n}\left(\tau,\nu|\tau',\nu'\right) \\ &\quad= h_{\mathrm{dd}}^{\mathrm{opt}} *_\sigma C_{\mathcal{Z}_n}\left(\tau,\nu|\tau',\nu'\right) \end{aligned} \tag{101}$$

Similarly, the noise covariance function for $h^\dagger *_\sigma n_{\mathrm{dd}}^{\mathrm{tf}}(\tau,\nu) := h^\dagger *_\sigma (g^{\mathrm{Tx}})^\dagger *_\sigma \mathcal{Z}_n(\tau,\nu)$ is given by

$$\begin{aligned} &C_{h^\dagger *_\sigma n_{\mathrm{dd}}^{\mathrm{tf}}}\left(\tau,\nu|\tau',\nu'\right) \\ &\quad= h^\dagger *_\sigma \left(g^{\mathrm{Tx}}\right)^\dagger *_\sigma g^{\mathrm{Tx}} *_\sigma h *_\sigma C_{\mathcal{Z}_n}\left(\tau,\nu|\tau',\nu'\right) \\ &\quad\approx h^\dagger *_\sigma h_{\mathrm{dd}}^{\mathrm{tf}} *_\sigma C_{\mathcal{Z}_n}\left(\tau,\nu|\tau',\nu'\right) \end{aligned} \tag{102}$$

from Lemma 2. Hence, the covariance functions are identical by (99) and (101). ■

REFERENCES

[1] R. Hadani et al., "Orthogonal time frequency space modulation," in *Proc. IEEE Wireless Commun. Netw. Conf. (WCNC)*, 2017, pp. 1–6.

[2] R. Hadani and A. Monk, "OTFS: A new generation of modulation addressing the challenges of 5G," 2018, *arXiv:1802.02623*.

[3] S. K. Mohammed, "Derivation of OTFS modulation from first principles," *IEEE Trans. Veh. Technol.*, vol. 70, no. 8, pp. 7619–7636, Aug. 2021.

[4] P. Raviteja, K. T. Phan, Y. Hong, and E. Viterbo, "Interference cancellation and iterative detection for orthogonal time frequency space modulation," *IEEE Trans. Wireless Commun.*, vol. 17, no. 10, pp. 6501–6515, Oct. 2018.

[5] P. Raviteja, K. T. Phan, and Y. Hong, "Embedded pilot-aided channel estimation for OTFS in delay-Doppler channels," *IEEE Trans. Veh. Technol.*, vol. 68, no. 5, pp. 4906–4917, May 2019.

[6] S. K. Mohammed, "Time-domain to delay-Doppler domain conversion of OTFS signals in very high mobility scenarios," *IEEE Trans. Veh. Technol.*, vol. 70, no. 6, pp. 6178–6183, Jun. 2021.

[7] S. K. Mohammed, R. Hadani, A. Chockalingam, and R. Calderbank, "OTFS—A mathematical foundation for communication and radar sensing in the delay-Doppler domain," *IEEE BITS Inf. Theory Mag.*, vol. 2, no. 2, pp. 36–55, Nov. 2022.

[8] S. K. Mohammed, R. Hadani, A. Chockalingam, and R. Calderbank, "OTFS—Predictability in the delay- doppler domain and its value to communication and radar sensing," *IEEE BITS Inf. Theory Mag.*, early access, Sep. 27, 2023, doi: 10.1109/MBITS.2023.3319595.

[9] S. Gopalam, I. B. Collings, S. V. Hanly, H. Inaltekin, S. R. B. Pillai, and P. Whiting, "Zak-OTFS implementation via time and frequency windowing," *IEEE Trans. Commun.*, early access, Feb. 14, 2024, doi: 10.1109/TCOMM.2024.3366403.

[10] H. Lin and J. Yuan, "Orthogonal delay-Doppler division multiplexing modulation," *IEEE Trans. Wireless Commun.*, vol. 21, no. 12, pp. 11024–11037, Dec. 2022.

[11] F. Lampel, H. Joudeh, A. Alvarado, and F. M. Willems, "Orthogonal time frequency space modulation based on the discrete Zak transform," *Entropy*, vol. 24, no. 12, p. 1704, 2022.

[12] S. Gopalam, S. B. Pillai, P. Whiting, H. Inaltekin, I. B. Collings, and S. V. Hanly, "A new micro-subcarrier OFDM based waveform for delay doppler domain communication," *IEEE Access*, vol. 12, pp. 57879–57894, 2024.

[13] M. Ubadah, S. K. Mohammed, R. Hadani, S. Kons, A. Chockalingam, and R. Calderbank, "Zak-OTFS for integration of sensing and communication," 2024, *arXiv:2404.04182*.

[14] R. G. Gallager, *Stochastic Processes: Theory for Applications*. Cambridge, U.K.: Cambridge Univ. Press, 2013.

[15] J. Proakis and M. Salehi, *Digital Communications*, 5th ed. New York, NY, USA: McGraw-Hill Higher Educ., 2008.

[16] Y. Ge, Q. Deng, P. C. Ching, and Z. Ding, "Receiver design for OTFS with a fractionally spaced sampling approach," *IEEE Trans. Wireless Commun.*, vol. 20, no. 7, pp. 4072–4086, Jul. 2021.

[17] P. Priya, E. Viterbo, and Y. Hong, "Low complexity MRC detection for OTFS receiver with oversampling," *IEEE Trans. Wireless Commun.*, vol. 23, no. 2, pp. 1459–1473, Feb. 2024.

[18] N. Hashimoto, N. Osawa, K. Yamazaki, and S. Ibi, "Channel estimation and equalization for CP-OFDM-based OTFS in fractional doppler channels," in *Proc. IEEE Int. Conf. Commun. Workshops (ICC Workshops)*, 2021, pp. 1–7.

[19] F. Liu, Z. Yuan, Q. Guo, Z. Wang, and P. Sun, "Message passing-based structured sparse signal recovery for estimation of OTFS channels with fractional doppler shifts," *IEEE Trans. Wireless Commun.*, vol. 20, no. 12, pp. 7773–7785, Dec. 2021.

[20] Z. Wei, W. Yuan, S. Lit, J. Yuant, and D. W. Kwan Ngt, "A new off-grid channel estimation method with sparse Bayesian learning for OTFS systems," in *Proc. IEEE Glob. Commun. Conf. (GLOBECOM)*, 2021, pp. 1–7.

[21] W. Yuan, Z. Wei, J. Yuan, and D. W. K. Ng, "A simple variational Bayes detector for orthogonal time frequency space (OTFS) modulation," *IEEE Trans. Veh. Technol.*, vol. 69, no. 7, pp. 7976–7980, Jul. 2020.

[22] H. Qu, G. Liu, L. Zhang, S. Wen, and M. A. Imran, "Low-complexity symbol detection and interference cancellation for OTFS system," *IEEE Trans. Commun.*, vol. 69, no. 3, pp. 1524–1537, Mar. 2021.

[23] F. Liu, Z. Yuan, Q. Guo, Z. Wang, and P. Sun, "Multi-block UAMP-based detection for OTFS with rectangular waveform," *IEEE Wireless Commun. Lett.*, vol. 11, no. 2, pp. 323–327, Feb. 2022.

[24] Z. Ye, S. Yan, Z. Sui, H. Zhang, and S. Sun, "Successive interference cancellation aided bidirectional soft decision feedback Equalization for OTFS systems," *IEEE Wireless Commun. Lett.*, vol. 12, no. 12, pp. 2028–2032, Dec. 2023.

[25] X. Li, H. Wang, Y. Ge, X. Shen, and J. Zhao, "Message feedback interference cancellation aided UAMP iterative detector for OTFS systems," *IEEE Wireless Commun. Lett.*, vol. 13, no. 4, pp. 924–928, Apr. 2024.

SWAROOP GOPALAM (Member, IEEE) received the B.Tech. degree in electrical engineering from the Indian Institute of Technology Bombay in 2014, and the M.Res. and Ph.D. degrees in engineering from Macquarie University, Sydney, Australia, in 2017 and 2021, respectively.

He has been working as a Research Fellow with the School of Engineering, Macquarie University since 2021. His research interests include delay-Doppler domain communication, resource allocation in wireless networks, and design of distributed and low-complexity algorithms.

HAZER INALTEKIN (Member, IEEE) received the B.S. degree (High Hons.) in electrical and electronics engineering from Bogazici University, Istanbul, Turkey, and the M.S. and Ph.D. degrees in electrical and computer engineering from Cornell University, Ithaca, NY, USA. He is a Senior Lecturer with Macquarie University. Prior to joining Macquarie University, he held various researcher and faculty positions in Australia, Europe, and USA. His research interests include airborne networks, satellite communications, fog/edge computing, IoT, wireless communications, and information theory.

IAIN B. COLLINGS (Fellow, IEEE) received the Ph.D. degree in systems engineering from Australian National University in 1995. He is a Professor with the School of Engineering, Macquarie University, Sydney, Australia. Previously, he spent nine years with CSIRO, where he held a number of roles, including the Deputy Chief of Division, a Research Program Leader, and a Theme Leader, and nine years with the Universities of Melbourne and Sydney. He has published over 300 papers in the area of wireless communications. He was awarded the Engineers Australia IREE Neville Thiele Award in 2009 and the IEEE CommSoc Stephen O. Rice Award in 2011. He has served as an Editor for IEEE TRANSACTIONS ON WIRELESS COMMUNICATIONS.

STEPHEN V. HANLY (Fellow, IEEE) received the Ph.D. degree in mathematics from Cambridge University, U.K., in 1994. He is a Professor with the School of Engineering, Macquarie University, Sydney, Australia. His research contributions are in wireless communications. He is a recipient of the INFOCOM Best Paper Award, the IEEE Information Theory Society and the IEEE Communication Society Joint Paper Award, and the IEEE Communications Society Tutorial Paper Award. He has been an Associate Editor of the IEEE TRANSACTIONS ON WIRELESS COMMUNICATIONS and a Guest Editor of the IEEE JOURNAL ON SELECTED AREAS IN COMMUNICATIONS. He has taken major roles at several IEEE conferences and workshops, including IEEE ISIT and IEEE CTW.